HYDRODYNAMICS OF THE SURF ZONE

IB A. SVENDSEN

RESEARCH REPORT NO. CACR-94-07

February 1994

CENTER FOR APPLIED COASTAL RESEARCH

Ocean Engineering Laboratory
University of Delaware
Newark, Delaware 19716

Contents

List of Figures

1 INTRODUCTION

Surf zone dynamics is a highly complicated topic in hydrodynamics which deals with the waves and wave generated phenomena in the region between the breaker line on a beach and the shoreline.

When waves break on a gently sloping beach, large amounts of energy are released and turned into turbulence. As the waves keep breaking and interacting with the bottom topography, the momentum flux of the waves also decreases along with the decrease in wave height. The forcing this represents causes the generation of both currents and longer waves.

The proper analysis of the dynamics of the surf zone requires a detailed knowledge of the breaking waves and the turbulence they create. This knowledge is not yet available. However, significant progress has been made over the last decade or two, in particular, in the area of understanding wave generated phenomena such as wave set-up, cross-shore and longshore currents and their stability, turbulence and mixing, and the generation of long wave phenomena (surf beats, edge waves), also termed infragravity waves.

The present chapter gives a brief account of the basic mechanisms involved in these phenomena.

Since the phenomena listed are all generated by the waves, and in most cases particularly by the forces released by the breaking process, it is evident that a proper description of the breaking waves in the surf zone is of crucial importance for an understanding of these phenomena.

We therefore start with an examination of the basic equations for nearshore circulation (Section 2) in which we also identify the wave properties (notably the mass flux, radiation stress, energy flux and energy dissipation due to breaking) responsible for the phenomena we want to study. In Section 3, a brief review is given of the status of our knowledge of those wave properties for breaking waves.

Section 4 reviews important examples of the simplest nearshore models that only predict wave heights and set-up, and in Section 5 the classical ideas of longshore and cross-shore currents are examined. That section also briefly covers more general circulation models. Finally, in Section 6 long wave generation (surf beat, edge waves) is examined and in Section 7 we discuss the recently discovered phenomenon of very long period waves [the so-called shear waves] that are believed to be signatures of instabilities of longshore currents.

Since the topic of surf zone hydrodynamics is very extensive, some of the subjects are merely covered in a brief descriptive way which primarily aims at referring the reader to relevant literature.

2 THE BASIC EQUATIONS OF NEARSHORE CIRCULATION

2.1 Introduction and Assumptions

The equations describing the wave generated currents and long wave motions in the nearshore region are based on the classical principles of hydrodynamics of conservation of mass, momentum and energy. Also, the exact boundary conditions at the bottom and the free surface are utilized. In order to cast the equations in a useful form for the purpose of studying nearshore circulation, the basic equations are first integrated over depth and thereafter averaged over a wave period. The results of this process will be discussed in the following to the extent that they are needed for the applications to be examined later. The reader interested in the detailed derivations is referred to Phillips (1980) (whose nomenclature and definitions we will largely follow) or Mei (1983) (who gives a somewhat more detailed account but whose definition of current differs at a crucial point from the one used here and by Phillips).

The amount of information supplied by these time averaged models is actually surprising. Properly formulated they can predict the wave height variation due to an assessed energy dissipation, the currents generated by the waves and also by the wind if we want to include that effect in the model. We also get information about the mean water surface (MWS) which is an important parameter in the nearshore balance. The wave averaged models can also predict long wave generation and behavior which is one of the most important topics in coastal research today.

Basic Assumptions

In order to be able to do the time (or wave) averaging, we need to assume that the (local) time (or "phase") variation of the wave motion is known. A typical example is the assumption that this variation is sinusoidal (though, unfortunately, that particular assumption is not a very good approximation for the breaking waves in a surf zone as we shall see).

The wave averaged models are also based on the assumption that the depth varies gently, as is the case almost (but not quite) everywhere on sandy shores and beaches.[1] The gentleness required is used to assume that at each location of the region the local wave motion corresponds to the wave motion we would have had at that location had the water depth been constant everywhere with exactly the local depth, and the wave height and wave period equal to the local values.

It turns out that this concept of gentleness is related both to the bottom slope h_x and to the wavelength L. Analysis of the effect the bottom has on the wave motion shows that to the first order this effect is proportional to the dimensionless ratio

$$S = \frac{h_x L}{h} \tag{2.1}$$

[1]Strictly speaking, this is not a necessary assumption but it highly simplifies the problems.

Since $h_x\ L = \Delta h$ is the (first Taylor approximation to the) change in depth over one wave length, we see that S is the *relative* change in depth over that distance.

Hence, we may conclude that if we want to be able to *neglect* the effect which a sloping bottom has on the local wave motion (i.e., to assume "locally constant depth"), we should assume conditions that everywhere satisfy the requirement that

$$S \ll 1 \tag{2.2}$$

This will also ensure that the assumption of no reflection of wave energy by the bottom topography is reasonable. In practice this usually is assumed to be satisfied if $S \leq 1$ though form some results $S < 0.3$–0.5 is probably necessary.

The locally-constant-depth assumption has tremendous advantages because it permits us to use known constant depth theories such as linear wave theory or Boussinesq long wave theory to describe the local details of the wave motion. All we need then is to determine the values of the wave parameters required to specify the waves according to those theories (such as wave height, H, period, T, wave direction, α, etc.) and that is exactly the information we get from the time averaged models.

In fact, the majority of all nearshore models fall short of achieving a satisfactory description of the wave and current phenomena because, as we will see, there are many complications and inadequacies in our knowledge of even the locally-constant-depth phase motion of the waves. This particularly applies to waves in the surf zone, and unfortunately this is, at the same time, the region which is most important for the littoral processes and the development of the coastal stability.

2.2 The Equations

It is convenient to some extent to use tensor notation for the final form of the equations. Usually, in tensor form a vector $\vec{v}$ is denoted v_i ($i = 1, 2, 3$). Since after the depth integration, however, only the horizontal coordinates (x, y) are left in the equations, the usual indices i, j will be replaced in depth integrated equations by α, β, where it is understood that α, $\beta = 1, 2$ only.

An important element in the analysis is the separation of the velocity components in a current component, which is termed by U, V, W, an oscillatory part (the "wave") denoted u_w, v_w, w_w, and a turbulent fluctuation denoted u', v', w'. Thus the total velocity components u, v, w are assumed to be the sum of those three components.

$$\begin{aligned} u &= U + u_w + u' \\ v &= V + v_w + v' \\ w &= 0 + w_w + w' \end{aligned} \tag{2.3}$$

where $W = 0$ has been assumed. This means we are neglecting the small vertical current that is typically present. Fig. 1 shows the notation used in the following.

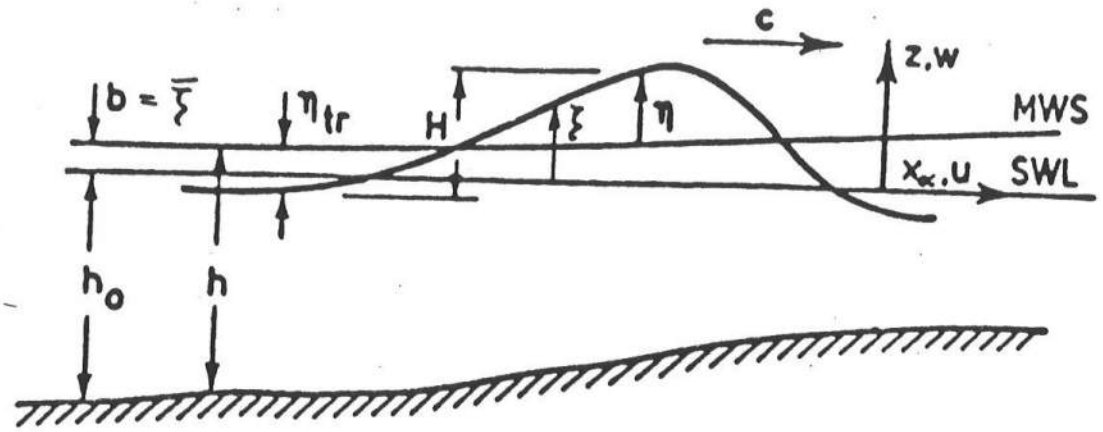

Figure 1: Notation.

Since the flow we are dealing with in the surf zone is generally so intensively turbulent from the wave breaking, the starting point for the derivations are the Reynolds equations for turbulent flow. We therefore also define the Reynolds (or "turbulent") averaged velocities as

$$\begin{aligned} \widehat{u} &= U + u_w \\ \widehat{v} &= V + v_w \\ \widehat{w} &= w_w \end{aligned} \tag{2.4}$$

In describing the result of the wave- (or time-) averaging we use $\overline{}$ to indicate time averaging, which means that

$$\bar{\cdot} = \frac{1}{T}\int_0^T \cdot\, dt \tag{2.5}$$

where T is the wave period.

We also assume (incorrectly!) that the current is constant over depth. The equations for a depth varying current are not only much more complicated algebraically but involve some conceptual complications that we want to avoid here. They will be briefly mentioned in Section 5 in the discussion of mixing.

Finally, we introduce the definition of the discharge or volume flux Q_α in the (horixontal) α-direction given by

$$Q_\alpha = \overline{\int_{-h_o}^{\zeta} U_\alpha + u_w \, dz} \tag{2.6}$$

Q_α is the total volume flux of water through a vertical section of unit width. For a depth uniform current this becomes

$$Q_\alpha = U_\alpha h + Q_{w\alpha} \tag{2.7}$$

where $Q_{w\alpha}$ is the volume flux due to the waves only. h is the total water depth.

$$h = h_0 + \bar{\zeta} (\equiv h_0 + b) \tag{2.8}$$

[Note that throughout this treatise both b and $\overline{\zeta}$ are used to describe the mean surface elevation.]

Continuity Equation

The final equation for conservation of mass (or rather volume since we assume the water incompressible) is then

$$\frac{\partial \overline{\zeta}}{\partial t} + \frac{\partial Q_\alpha}{\partial x_\alpha} = 0 \tag{2.9}$$

where the so-called "summation rule" is understood which means $\frac{\partial Q_\alpha}{\partial x_\alpha} = \frac{\partial Q_x}{\partial x} + \frac{\partial Q_y}{\partial y}$. (2.9) essentially says that a net change in the x, y directions of the total time averaged discharge Q_α will result in a change in mean water elevation $\overline{\zeta}(= b)$.

Horizontal Momentum Equations

Similarly, the horizontal momentum equation becomes

$$\rho \frac{\partial Q_\alpha}{\partial t} + \frac{\partial}{\partial x_\beta}\left(\rho \frac{Q_\alpha Q_\beta}{h} + S_{\alpha\beta} + S'_{\alpha\beta}\right) = -\rho\, g h \frac{\partial \overline{\zeta}}{\partial x_\alpha} + \tau_\alpha^S - \tau_\alpha^B \tag{2.10}$$

again with summation over β assumed in the second term. Equation (2.10) (which actually represents an x and a y component) introduces several new concepts.

In particular, $S_{\alpha\beta}$ is the so-called radiation stress which represents the net (time averaged) force the waves excert on a water column.

Similarly, $S'_{\alpha\beta}$ is the net effect of the turbulent stresses; τ_α^S would represent any shear stress on the free surface due to, e.g., wind; and τ_α^B is the mean bottom shear caused by the combined wave-current motion.

The physical significance of the terms in (2.10) will be discussed further in Sections 5 and 6. The assessment of the turbulent stress term $S'_{\alpha\beta}$ and the mean bottom shear stress is also discussed further in Section 5. Here we limit the discussion to examining closer the definition of the radiation stress.

The Radiation Stress, $S_{\alpha\beta}$

The radiation stress, $S_{\alpha\beta}$ is a short notation for a number of terms that emerge from the derivation of (2.10). Thus $S_{\alpha\beta}$ is defined as

$$\begin{aligned} S_{\alpha\beta} &= \overline{\int_{-h_o}^{\zeta} \rho\left(u_{w\alpha}u_{w\beta} - \delta_{\alpha\beta}\left(w^2 + \widehat{w'^2}\right)dz\right)} \\ &\quad + \frac{1}{2}\delta_{\alpha\beta}\rho\, g\, \overline{\eta^2} - \rho\frac{Q_{w\alpha}Q_{w\beta}}{h} \end{aligned} \tag{2.11}$$

where $\eta = \zeta - \bar{\zeta}$ is the water surface variation measured relative to the mean water surface. $\delta_{\alpha\beta}$ is the Kroenecker symbol (which is 1 if $\alpha = \beta$, 0 if $\alpha \neq \beta$). Written out in x, y coordinates, $S_{\alpha\beta}$ has the following four components:

$$S_{xx} = \overline{\int_{-h_o}^{\zeta} \rho\left(u_w^2 - \left(w_w^2 + \widehat{w'^2}\right)\right)dz} + \frac{1}{2}\rho\, g\overline{\eta^2} - \rho\frac{Q_{wx}^2}{h} \tag{2.12}$$

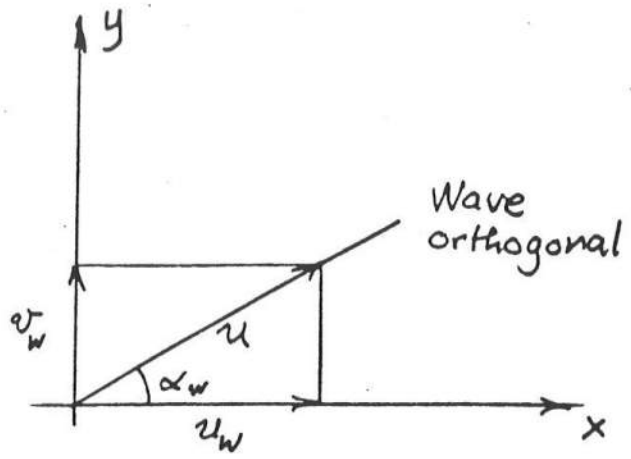

Figure 2: Wave propagating at an angle α_w to the x- axis.

$$S_{xy} = S_{yx} = \overline{\int_{-h_o}^{\zeta} \rho\, u_w\, v_w\, dz} - \rho \frac{Q_{wx} Q_{wy}}{h} \tag{2.13}$$

$$S_{yy} = \overline{\int_{-h_o}^{\zeta} \rho \left(v_w^2 - \left(w_w^2 + \widehat{w'^2} \right) \right) dz} + \frac{1}{2} \rho\, g \overline{\eta^2} - \rho \frac{Q_{wy}^2}{h} \tag{2.14}$$

The Q_w-terms are is usually considered small. If we deal with linear waves, they are $O(H^4)$ which is small relative to the magnitude of $S_{\alpha\beta}$, which is $O(H^2)$. In the surf zone, however, this is not always the case.

In order to further understand the concept of radiation stress, we look at an example where a wave approaches a shore and propagates at an angle α_w with the x axis. Fig. 2 shows the situation. In the vertical plane of the wave direction the wave-induced particle velocities are

$$u = (u_w^2 + v_w^2)^{1/2} \tag{2.15}$$

$$w = w_w \tag{2.16}$$

and discharge is

$$Q_w = (Q_{wx}^2 + Q_{wy}^2)^{1/2} \tag{2.17}$$

We then define (the scalars)

$$S_m = \overline{\int_{-h_o}^{\zeta} \rho u^2\, dz} - \rho \frac{Q_w^2}{h} \tag{2.18}$$

$$S_p = -\overline{\int_{-h_o}^{\zeta} \rho\, w^2 + \widehat{w'^2} dz} + \frac{1}{2} \rho g \overline{\eta^2} \tag{2.19}$$

so that

$$S_r = S_m + S_p \tag{2.20}$$

represents the radiation stress on a vertical surface with the normal vector in the direction of wave propagation.

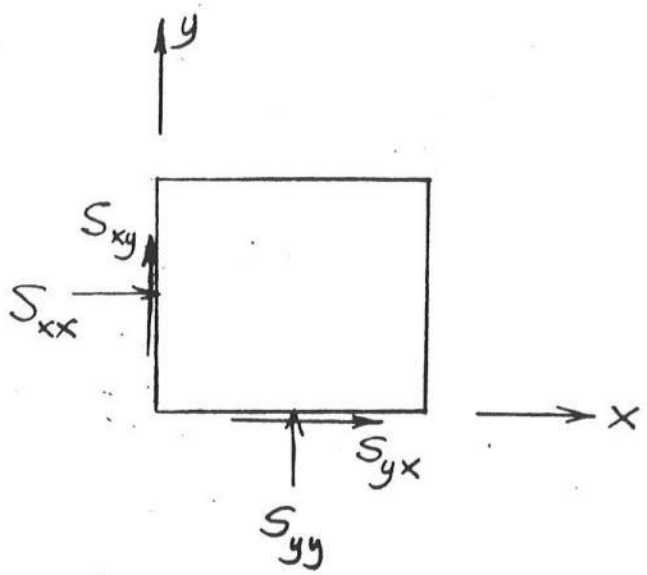

Figure 3: Radiation stress components in different directions. Notice positive directions are opposite normal stresses.

Then the four components of $S_{\alpha\beta}$ that represents the radiation stress elements parallel and perpendicular to the x, y axes can be written

$$S_{xx} = S_m \cos^2 \alpha_w + S_p \tag{2.21}$$

$$S_{xy} = S_{yx} = S_m \sin \alpha_w \cos \alpha_w \tag{2.22}$$

$$S_{yy} = S_m \sin^2 \alpha_w + S_p \tag{2.23}$$

Fig. 3 shows the situation described by these expressions. Thus, if we define $e_{\alpha\beta}$ as the matrix

$$e_{\alpha\beta} = \left\{ \begin{array}{ll} \cos^2 \alpha_w & \sin \alpha_w \cos \alpha_w \\ \sin \alpha_w \cos \alpha_w & \sin^2 \alpha_w \end{array} \right\} \tag{2.24}$$

we can write $S_{\alpha\beta}$ in the simple form

$$S_{\alpha\beta} = S_m \, e_{\alpha\beta} + S_p \delta_{\alpha\beta} \tag{2.25}$$

Hence, it is possible from the results S_m and S_p for the radiation stress components on a surface perpendicular to the direction of wave propagation to determine the radiation stress $S_{\alpha\beta}$ in any direction.

Note that all results obtained so far apply for any periodic wave train, including surf zone waves.

The evaluation of $S_{\alpha\beta}$ for surf zone waves is discussed in Section 3.

For reference, however, it is noticed that for linear (or "sine") waves, we get

$$S_m = \frac{1}{16} \rho \, g \, H^2 (1 + G) \tag{2.26}$$

$$S_p = \frac{1}{16} \rho \, g \, H^2 \, G \tag{2.27}$$

where $G \equiv 2kh/\sinh 2kh$, and $k = 2\pi/L$ is the wave number.

The Energy Equation

Also the energy equation for the combined wave and current motion is needed in wave averaged models and can be derived by the same depth integration and time averaging process. In its general form, the energy equation is even more complicated than the momentum equation (2.10).

Reference is made to Phillips (1980). However, the current terms in the energy equation are usually of minor importance for the simple applications discussed here. We, therefore, restrict the discussion to the simplified version for wave motion only, which reads

$$\frac{\partial E_{f,\alpha}}{\partial x_\alpha} = \mathcal{D} \tag{2.28}$$

Here, $E_{f\alpha}$ is the energy flux of the waves in the α direction and $\mathcal{D}$ is the energy dissipation per unit time and area of bottom.

As in the momentum equation, the energy flux for the waves is an abbreviation for a number of terms that emerge through the derivation of the equation. It is defined as

$$E_{f\alpha} = \overline{\int_{-h_o}^{\zeta} \left(\rho\, g z + p + \frac{1}{2}\rho(u_w^2 + v_w^2 + w_w^2)\right) u_{w\alpha}\, dz} \tag{2.29}$$

For sine waves (2.29) yields

$$E_f = \frac{1}{16}\,\rho\, g\, lc\, H^2(1+G) \tag{2.30}$$

The dissipation of energy $\mathcal{D}$ can be described by the work done by internal (turbulent) stresses, but this does not lead to a viable means of determining $\mathcal{D}$ from our present knowledge of the wave motion.

Note that energy dissipation (2.28) corresponds to $\mathcal{D} < 0$. The practical evaluation of $E_{f,\alpha}$ and $\mathcal{D}$ is discussed in more detail in Sections 3 and 4.

General Use of the Equation

Basically, solution of the energy equation will supply information of the variation of the wave height, H, whereas solution of the continuity and momentum equations are providing information about water level variations $h(=\bar{\zeta})$ and currents. Examples of the latter will be given in Sections 5 and 6, whereas, determination of the wave height and set-up is discussed in Section 4.

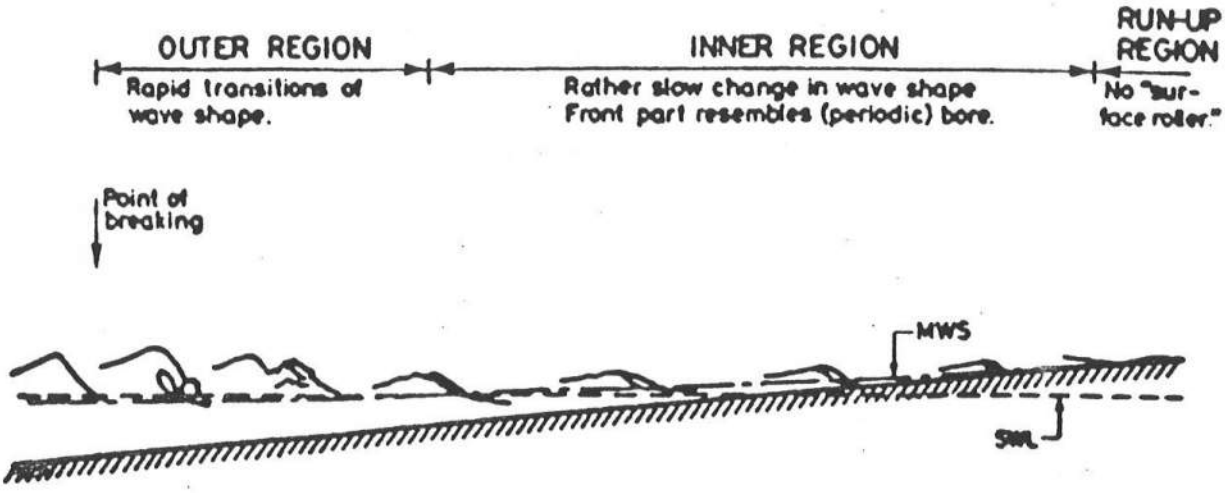

Figure 4: Wave characteristics in the surf zone (from Svendsen et al., 1978).

3 THE WAVE MOTION

3.1 General Description

Fig. 4 shows a schematic of the wave motion from the breaker point of a gently sloping beach, as most littoral beaches are, to the shoreline. The waves may initially break in a range of different patterns that reach from the relatively controlled "spilling" to the violent and relatively sudden "plunging" breaker type, (Galvin 1968). In any type of breaking there will be a rapid and substantial change in the shape of the wave immediately following the initiation of breaking. This region has been termed the Outer or Transition Region, which covers a distance of, say 8–10 water depths after the breaker point (Svendsen et al., 1978).

Shoreward of the transition region, the wave shape and the general velocity field induced by the wave will change much more slowly. In this region, the broken waves have many features in common with bores. This is the so-called Inner or Bore Region which stretches all the way to the shore (or, if the breaking occurred on a longshore bar, till the waves stop breaking by passing into the deeper water shoreward of the bar).

On many natural beaches the foreshore is much steeper than the rest of the beach. In the run-up on the shore on such beaches (termed the swash zone), the wave motion often shows a different pattern from that of the rest of the surf zone.

3.2 The Transition Region

Very little has been published in the literature about the transition region. The results are almost entirely descriptive and based on photographic and optical methods. Basco and Yamashita (1986) gives an interpretation of the flow based on such information particularly for a plunging breaker and shows how the overturning of the wave creates patterns that look chaotic but are nevertheless largely repeated from wave to wave.

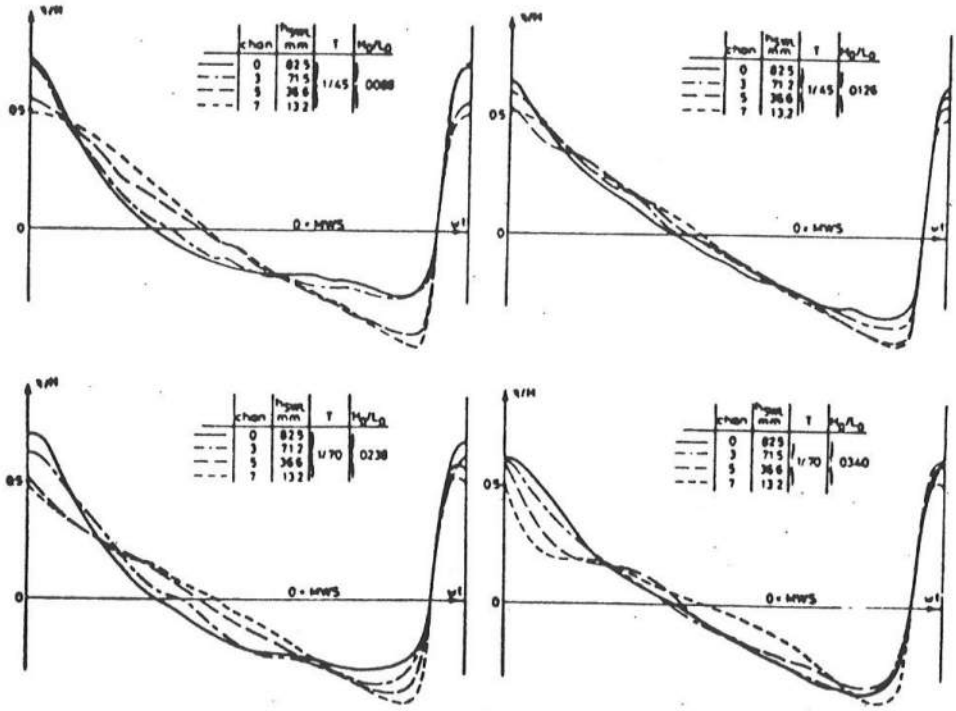

Figure 5: The development of wave profiles in the surf zone (from Svendsen et al., 1978).

Similar interpretations are given by Tallent et al. (1989), and Jansen (1986) has mapped the variation of the free surface in this region through high speed video recordings of fluorescent tracers. Finally, Okayasu (1989) gives detailed measurements of the entire velocity field in the transition region from experiments using laser doppler velocimetry. Those results have been obtained, however, by repeating the same experiments many times and each time averaging over several waves and therefore cannot quite be regarded as a picture of the instantaneous velocity field in a particular wave.

3.3 The Bore Region

Also in the Bore Region the information about the wave properties is almost entirely empirical since no predictive models of the actual wave motion have been developed so far. Knowledge about the waves in this region is far more extensive, however, than for the outer region.

Among the experimental results for the Bore Region it can be mentioned that Svendsen et al. (1978) found that the wave surface profiles would develop a relatively steep front with a much more gently sloping rear side. The shape of the surface profile on the rear side of the wave will develop from a concave towards an almost linear variation, so that near the shore of a gently sloping beach the wave is close to a sawtooth shape. Fig. 5 shows the tendency. Measurements of velocity fields using laser doppler velocimetry have been reported by Stive (1980), Stive and Wind (1982), Nadaoka (1986) and Okayasu (1989). In all cases, however, the measurements are limited to the regions away from the crest because none of the measuring techniques available today make it possible to measure velocities in the highly aerated region near the front of the breaker. That means

wave averaged quantities such as radiation stresses, S_r, and energy flux, E_f, which get significant contributions from those regions, can only be determined with limited accuracy on the basis of such measurements. Stive and Wind (1982) gives a detailed account of the problem.

Stive (1984) also analyzed data from his experiments to determine the energy dissipation, D, in surf zone waves extending a theoretical result developed by Svendsen et al. (1978) and Svendsen and Madsen (1981), and confirmed that the dissipation is likely to be up to 50% larger than in a bore of the same height. This will be discussed more explicitly in Section 3.5.

In many of the wave models, various characteristics of the wave motion are used as parameters. Examples are the rms of the surface profile, $B_0 = \overline{\eta^2}/H^2$; the wave propagation speed, c; the vertical skewness given as relative crest elevation, η_c/H, in addition to breaker data. Hansen (1990) analyzed original data from most of the detailed experiments quoted above and developed an empirical representation for those parameters that in most cases fit the data remarkably well.

For sine waves, $B_0 = 1/8 = 0.125$. For the surf zone waves, Hansen found the variation shown in Fig. 6, which is given by

$$B_0 = B_{0B}\,[1 - a(b - h/h_B)(1 - h/h_B)] \tag{3.1}$$

$$a = (15\xi_{00})^{-1} \;\; ; \;\; b = 1.3 = 1.0\,(\xi_0 - \xi_{00}) \tag{3.2}$$

$$\xi_0 = h_x/\sqrt{H_i/L_0} \;\; ; \;\; \xi_{00} = h_x/\sqrt{0.142} \tag{3.3}$$

$$B_{oB} = 0.125\tanh(11.40/\sqrt{U_B}) \tag{3.4}$$

$$U_B = 10h_x^{0.20}(H_0/L_0)^{-1} \tag{3.5}$$

Here H_0/L_0 is the deep water wave steepness and it is noted that ξ_0 is the so-called surf zone similarity parameter.

The results for the vertical skewness are shown in Fig. 7. The expressions describing the results are

$$\frac{\eta_c}{H} = 0.5 + \left[\left(\frac{\eta_c}{H}\right)_B - 0.5\right]\left(\frac{h}{h_B}\right)^2 \tag{3.6}$$

where

$$\left(\frac{\eta_c}{H}\right)_B = 1 - 0.5\tanh\left(4.85/\sqrt{U_B}\right) \tag{3.7}$$

with U_B given by (3.5).

These results are utilized in the following.

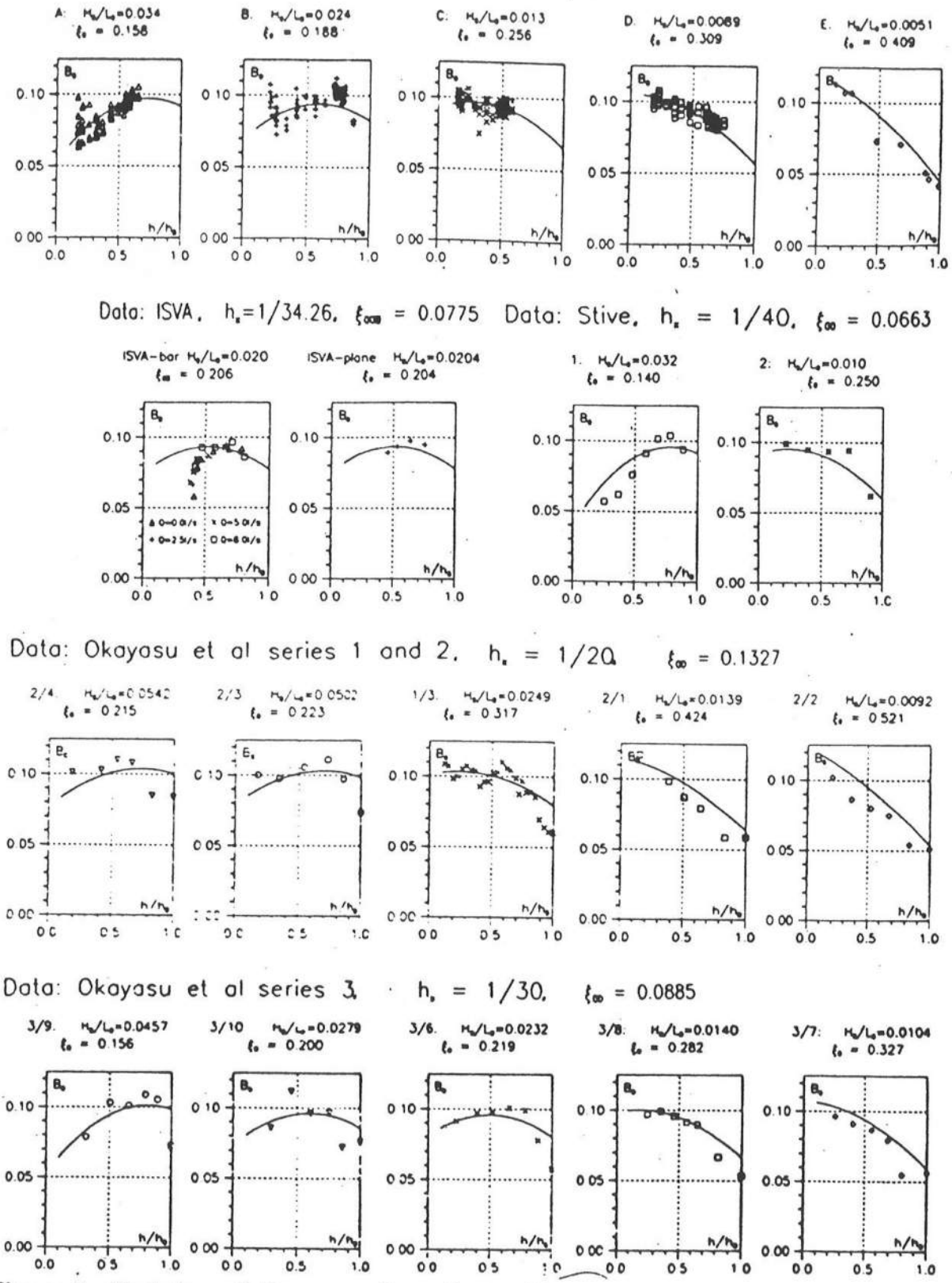

Figure 6: Variation of the wave shape factor B_0. — represents Eqs. 3.1–3.5 (from Hansen, 1990)

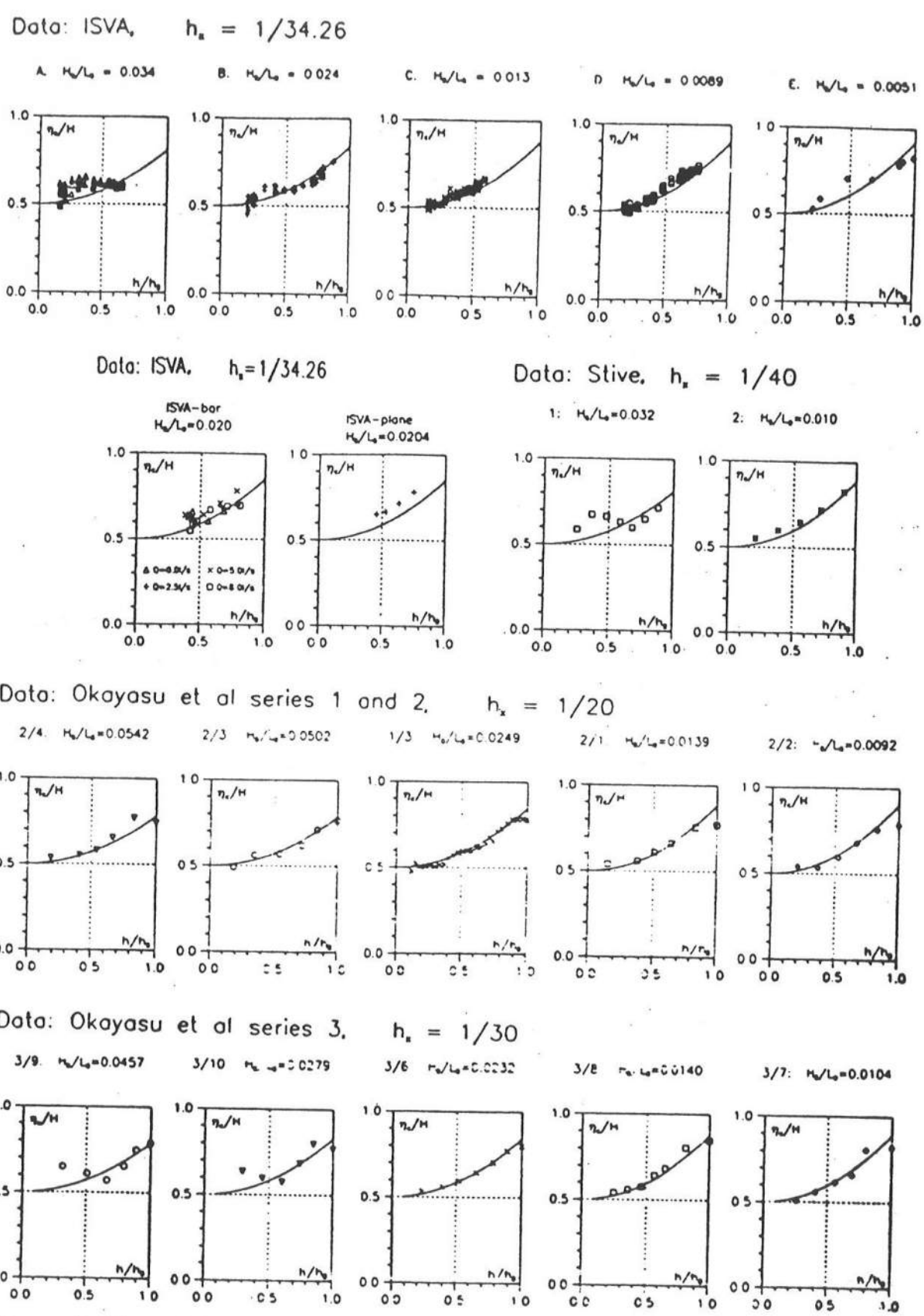

Figure 7: Vertical skewness η_c/H. — represents Eqs. 3.6–3.7 (from Hansen, 1990)

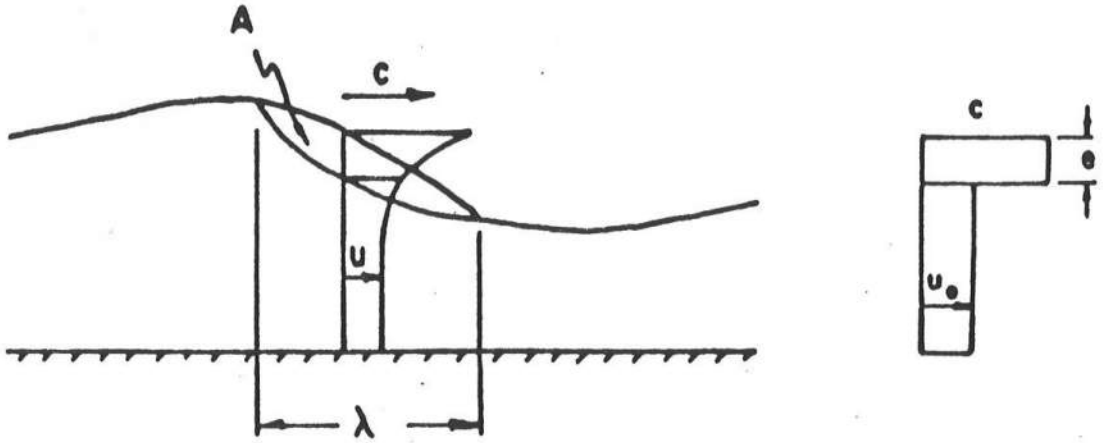

Figure 8: Surf zone waves with a roller (from Svendsen, 1984a).

3.4 The Main Wave Parameters

As we have seen in equations (2.9), (2.10) and (2.28) describing the wave generated current and long wave phenomena, the effects of the waves are essentially described by the volume flux, Q_w, due to the wave motion; the momentum flux or radiation stress, $S_{\alpha\beta}$; and the energy flux, $E_{f,\alpha}$. An additional, important wave averaged quantity is the energy dissipation $\mathcal{D}$ caused by the wave breaking. Therefore, to be able to predict nearshore circulation and longwave phenomena from the averaged models, these quantities must be expressed in terms of wave height, wave period, water depth, etc. for surf zone waves.

The wave model used by Svendsen (1984a) acknowledges that surf zone waves are non-sinusoidal long waves (length $\gg$ depth) and especially accounts for the fact that in breakers a volume of water, the so-called surface roller, is carried with the wave speed c. The situation is illustrated in Fig. 8. Using these assumptions, it is found that in the wave direction we have the radiation stress

$$S_r = S_m + S_p \qquad (2.20)$$

where

$$S_m = \rho\, g\, H^2 \left(B_0 + \frac{A}{H^2}\,\frac{c}{gT} \right) \qquad (3.8)$$

$$S_p = \frac{1}{2}\,\rho\, g\, H^2\, B_0 \qquad (3.9)$$

$$E_f = \rho\, g\, c\, H^2 \left(B_0 + \frac{1}{2}\,\frac{A}{H^2}\,\frac{c}{gT} \right) \qquad (3.10)$$

B_0 defined as

$$B_0 = \frac{\overline{\eta^2}}{H^2} \qquad (3.11)$$

represents the effect of the wave surface profile and may be determined from (3.1)–(3.5). A is the area of the surface roller in the vertical plane. A was measured by Duncan

(1981) and Svendsen (1984a) found the approximation $A/H^2 = 0.9$ constant over the surf zone based on Duncan's data. Later Okayasu (1989) has suggested that a more accurate expression may be $A/HL = 0.06$.

As may be deduced from (3.8)–(3.10), in the wave direction we can, without loss of generality, write the wave parameters the following way

$$Q = c\frac{H^2}{h}B_Q \tag{3.12}$$

$$S = \rho\, g\, H^2 P \tag{3.13}$$

$$E_f = \rho\, g\, c\, H^2 B \tag{3.14}$$

$$\mathcal{D} = g\,\frac{H^3}{4hT}D \tag{3.15}$$

Essentially, these expressions define dimensionless parameters B_Q, P, B and D for the four wave quantities. In a simplified manner, one can say that the dimensional components h, H, T and c in (3.11)–(3.15) measure the size of the wave motion, whereas the dimensionless parameters are measures of the shape of the wave motion (understood as surface profile, velocity and pressure field, etc.).

Both for the sine waves and for the surf zone wave model described above, the values of these dimensionless quantities can readily be determined. The question of how accurate they are is discussed below.

The energy dissipation due to breaking is often assumed equal to the dissipation in a hydraulic jump or bore of height H. Then the dimensionless dissipation D becomes

$$D = D_{\text{bore}} = \frac{h^2}{d_t\, d_c} \tag{3.16}$$

where d_t and d_c are the depths under the wave trough and wave crest, respectively (Svendsen et al., 1978). For most surf zone waves (3.16) gives values of $D_{\text{bore}} \sim 0.9$.

Direct Empirical Results for P, B and D

Clearly, the correct prediction or specification of B_Q, P, B and D is as important for the prediction of the averaged quantities Q_s, S, E_f and D as the wave H and water depth including set-up. The prediction of H is discussed in more detail in Section 4. Here we briefly concentrate on empirical results for P, B and D.

Recently, Putrevu & Svendsen (1991) used measurements of wave height and set-up from a large number of laboratory experiments to determine the actual values of P, B and D in surf zone waves. The results are shown in Figures 9, 10 and 11. In each case, the results are divided according to the scaled bottom slope S_B at the breaker point. S_B is defined as

$$S_B = \left(\frac{h_x L}{h}\right)_B \tag{3.17}$$

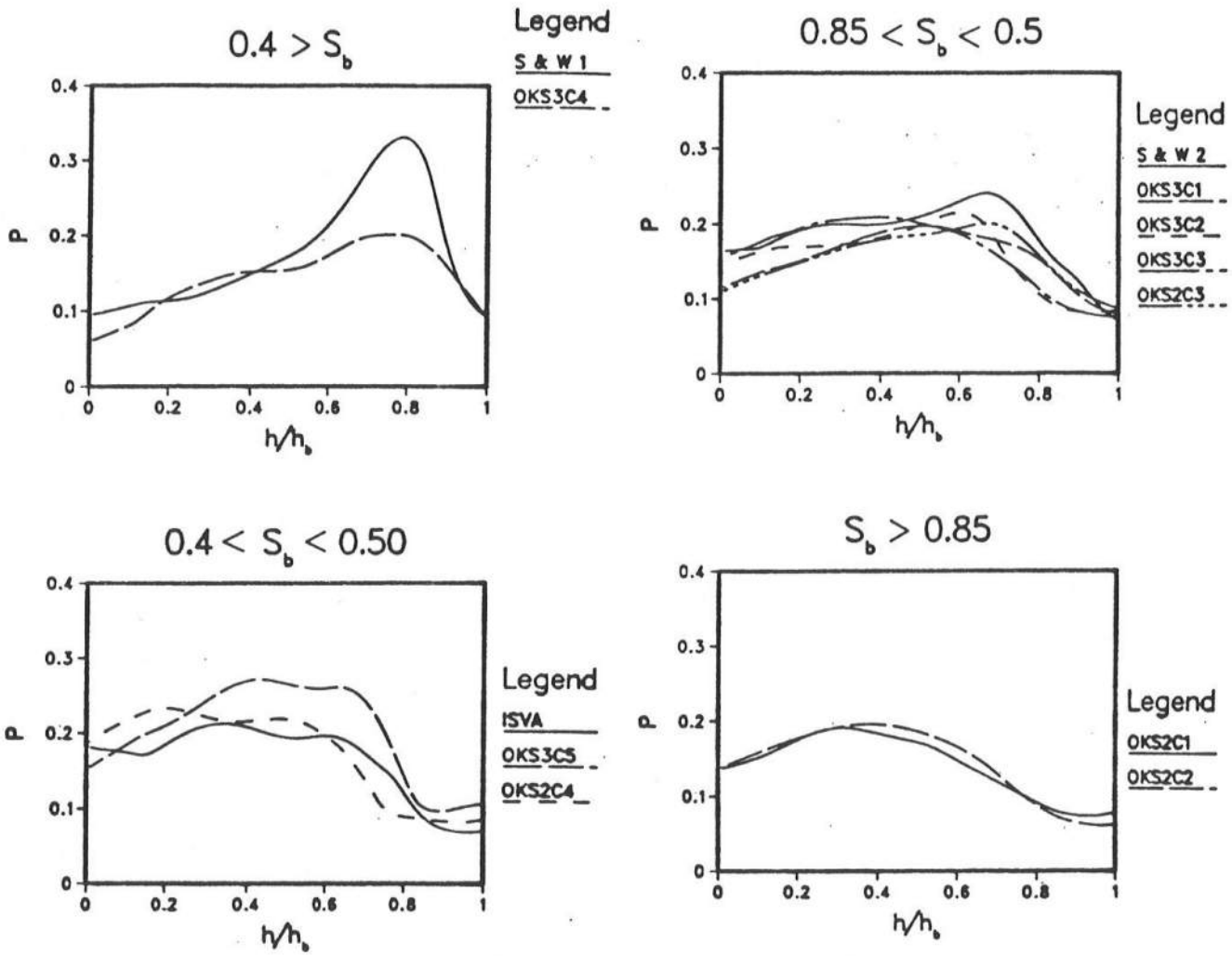

Figure 9: Variation of $P_{\sin}$ determined from experimental data.

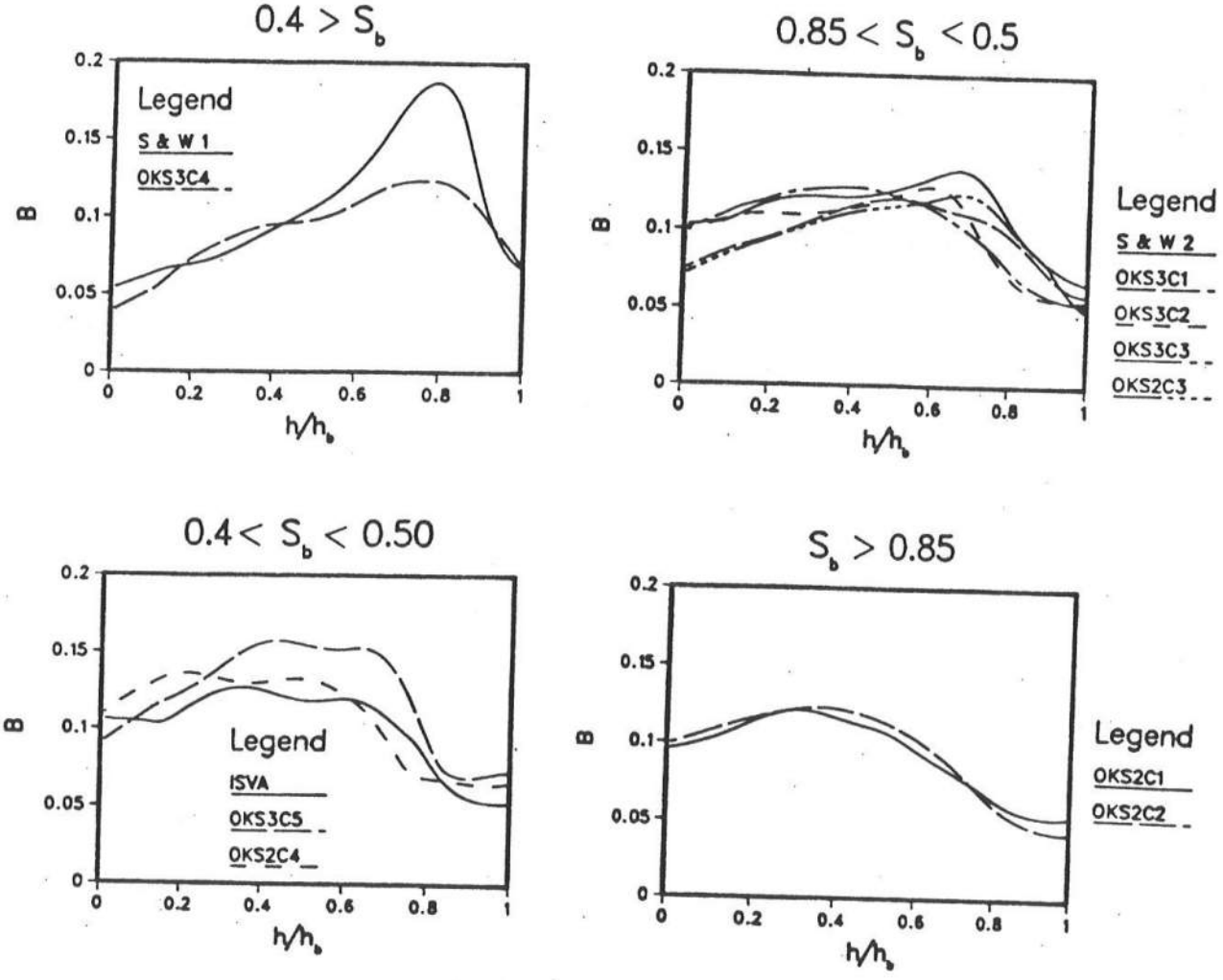

Figure 10: Variation of B determined from experimental data.

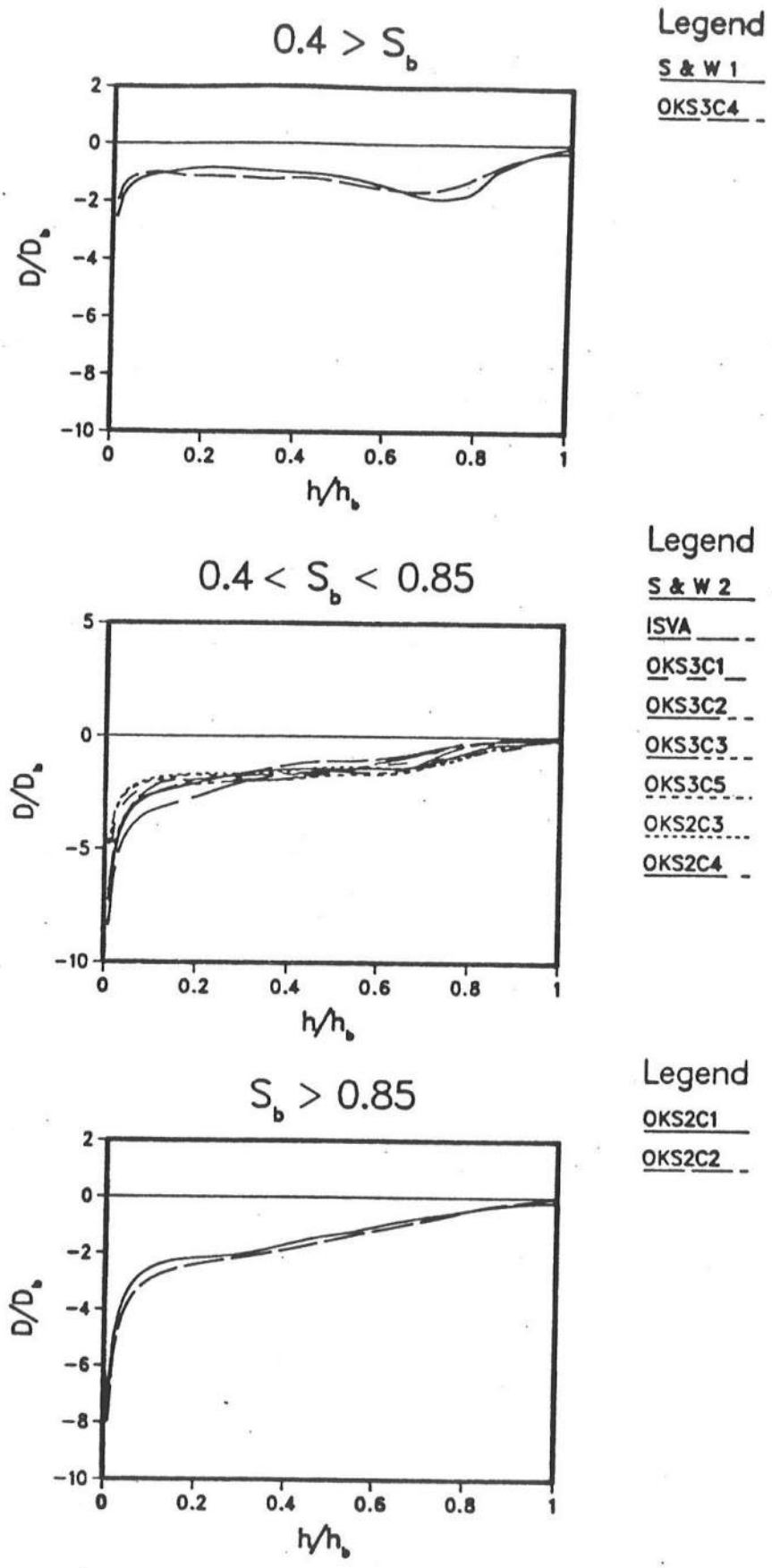

Figure 11: Variation of D determined from experimental data.

mentioned earlier. h_x is the bottom slope (constant) in the experiments, L the wave length and h_B the water depth at breaking.

In Figures 9 and 10 are also shown for reference the P and B values corresponding to the long wave limit of (2.26), (2.27) and (2.30); i.e., linear long wave theory.

Several important conclusions can be drawn from these figures

i. First the (not very surprising) conclusion that sine wave theory is inappropriate as approximation for P and B.

ii. The variation of the wave properties such as radiation stress, $S_{\alpha\beta}$ and energy flux, $E_{f,\alpha}$ clearly depend not only on the variation of the wave height, though that remains an important parameter. The variation of the wave shape represented by P and B is equally important for the correct prediction of radiation stress and energy flux.

iii. If the breaking were almost equal to that in a bore, we would have $D \sim D_{\text{bore}}$, that is $D \sim 1$. Clearly, in most cases the actual dissipation is substantially larger (from 50% to several hundred percent).

Notice that the sudden growth in D in the nearshore region in Figure 11 is more a consequence of the definition of D by (3.15) than growth in the physical dissipation $\mathcal{D}$. It simply signifies that near the shore there is little resemblance with the situations in a steady bore.

Turbulence

Peregrine and Svendsen (1978) found experimentally that the turbulence generated by the breaking, while initiated at the toe of the turbulent wave front, spreads downwards and continues to do so long after the breaker has passed. Pointing to the resemblance between spilling breakers and waves in the bore region of a surf zone, and bores and hydraulic jumps, they speculated that the spreading mechanism is similar to that in a shear layer.

Later, measurements by Battjes and Sakai (1981) indicated closer resemblance with the turbulence characteristics in a wake. The truth is that the turbulence generated by wave breaking and its dispersion is different from all other turbulent phenomena. The distribution of turbulent intensities below wave MWL was reported by Stive and Wind (1982), Nadaoka (1986), and in more detail by Okayasu (1989).

Data for breaker generated turbulence has also been provided by Hattori and Aono (1985) who found the turbulent energy spectra have large proportions of the energy at frequencies only somewhat higher than the wave frequency indicating the existence of large scale vortices. Nadaoka (1986) identified a regular system of vortices with axes sloping downwards from the free surface and developing at some distance behind the front.

Battjes (1975) and later Svendsen (1987) analyzed turbulent kinetic energies under breaking waves, and the latter found that most of the energy is actually dissipated in the crest above the MWL.

3.5 Other Model Results

The details of the highly turbulent area at the front (the so-called "roller") was analyzed by Longuet-Higgins and Turner (1974) who assumed that air entrainment played a vital part in maintaining this roller in position on the sloping front. Later results of experiments and analysis by Duncan (1981), Svendsen and Madsen (1984), Banner (1987) and Deigaard (1989) all in various ways attribute the support of the roller to turbulent shear stresses. Longuet-Higgins (1973) also analyzed the nature of the flow in the neighborhood of the toe of roller assuming a separation point here. An alternative flow pattern was used in the model developed by Svendsen and Madsen (1984).

4 2-D WAVE AND SET-UP MODELS

As shown in Section 3, the important wave parameters depend critically on the wave height H. Therefore, the prediction of H in particularly inside the surf zone becomes of particular importance for a successful modelling of all the wave generated nearshore phenomena. As will be clear, this prediction rests entirely on the correct assessment of B and D since with these parameters known H follows from the energy equation. It is therefore interesting to examine the performance of available models.

The simplest model for the wave height H assumes that in the surf zone H is a constant fraction of γ of the water depth (saturated breaker)

$$H = \gamma h \tag{4.1}$$

and invoking linear (sine wave) results for all the time averaged wave quantities. As we have seen, this is not a very accurate prediction, though it is sometimes meaningful when studying phenomena where the aim is the principal nature of the problem rather than an accurate prediction (such as the classical longshore current theories described in Section 5, and the simple analysis of set-up inside the surf zone described below).

Here we concentrate on the so-called H-b models which correspond to modelling the cross-shore wave averaged momentum and energy balance in the surf zone.

4.1 H-b Models

The H-b models essentially solve simplified versions of the momentum and energy equations (2.10) and (2.28) by considering only the simple 1D cross shore situation (long, straight coast, perpendicular wave incidence). These models also assume the currents to be weak, and neglect the small cross-shore mean bottom friction. The momentum and energy equations can then be written

Momentum:

$$\frac{d\,S_{xx}}{dx} = -\rho\, g(h_o + b)\,\frac{db}{dx} \tag{4.2}$$

Energy:

$$\frac{d\,E_{fx}}{dx} = \mathcal{D} \tag{4.3}$$

where S_{xx} and E_{fx} are given by (2.20) and (2.29), respectively.

Setdown and set-up

The simplest possible versions of H-b models are represented by the solutions to the momentum and energy equations (4.2) and (4.3) for two simplified cases.

i. Non-breaking sine-waves over a gently varying topography (Longuet-Higgins & Stewart, 1963).

ii. Waves, normally incident, breaking on a long, straight beach combined with the assumption that $H = \gamma\, h$ (Bowen et al., 1968).

In both cases, (4.2) can be solved analytically in spite of the fact that it is a nonlinear equation because it contains the term $b\, db/dx$.

In the first case, the solution to (4.2) is obtained by substituting (2.26) and (2.27) for S_m and S_p.

The result is

$$b = -\frac{1}{16}\frac{H^2}{h}\,G \tag{4.4}$$

in which (4.2) has also been utilized and therefore satisfied with $\mathcal{D} = 0$ (no energy dissipation).

It is recalled that b is the vertical distance from a chosen reference level ($z = 0$ in Fig. 1) to the mean water level (where $\bar{\eta} = 0$). (4.4) corresponds to $b = 0$ at deep water, and hence (4.4) shows that non-breaking waves create a depression of the mean water level ("setdown") as they propagate towards more shallow water. As (4.2) shows, this is a consequence of the increase in S_{xx} predicted by the linear theory as the depth decreases and the wave height increases. A further consequence of this is the fact that the largest value of the setdown occurs at the breaker point according to this theory (and measurements confirm that this is largely true).

In the situation ii), the energy equation (4.3) is replaced by the assumption (4.1) of wave heights that correspond to a constant fraction of the local water depth, and the long wave limit of (2.26)-(2.27) is used for S_{xx}. (4.2) can then be integrated directly which results in

$$b = \frac{-3\gamma^2}{8(1+\frac{3}{8}\gamma^2}\,(h_0(x) - h_{0B}) + b_B \tag{4.5}$$

where h_{0B} is the undisturbed depth at the breaking point and b_B is the setdown at the same location. In principle, b_B can be determined from (4.4).

As is evident from the discussion of the values of P and B, the setdown (4.4) and the set-up (4.5) cannot be very accurate because they are based on unrealistic assumptions for the wave height and for E_f and S_{xx}. The results for b, however, do qualitatively predict the basic feature that the setdown outside the surf zone is only of the order 1–10

cm even for large storm waves whereas the set-up near the shoreline can be O (1m) for large waves. If, for example, we assume $\gamma = 0.6$ (a typical value for surf zone waves) and neglect b_B, we find that at $h_0 = 0$ (the undisturbed shoreline), $b = 0.12 h_B$ or 12% of the water depth where the waves break.

The more realistic surf zone approximations for S_{xx}, $E_{f,x}$ and $\mathcal{D}$ suggested by Svendsen (1984a) were already described in Section 3.

The model by Dally et al. (1984) is particular by including an empirical threshold in the energy dissipation that let the waves stop breaking when their height to depth ratio becomes too small.

This has relevance to actual physical situations such as when a wave passes over the crest of a longshore bar into deeper water behind. The sudden increase in depth reduce the H/h ratio and the wave usually stops breaking. The model, however, has an empirical constant which is adjusted to fit experimental data for H. It also uses linear wave theory to predict the energy flux (i.e., B). Hence, the empirical constant absorbs the error in B and the actual numbers in the energy equation for energy flux and dissipation become similarly artificial although the wave height is well predicted. This shows in a less accurate performance of the model in predicting the set-up (i.e., the radiation stress) using the empirical calibration constant found for the wave height (Dally et al., 1985).

This inability to predict both wave height and set-up correctly is in fact characteristic of the presently known H-b models. Fig. 12 shows the performance of the two models described above for three different laboratory experiments. Stive & Wind (1982) (1:40), Okayasu (1988) (1:30) and Visser (1982,1984) (1:10,1:20).

Whereas the models are fairly capable of predicting the wave height variations, the accuracy in the prediction of the set-up is much less convincing, although the more realistic wave representation used by Svendsen is somewhat more accurate (in particular when combined with Hansen's B_0) than the two versions of Dally et al.'s models.

Fig. 13 shows a comparison with the actual P, B and $\mathcal{D}$ for four of the experiments.

4.2 Irregular Wave Models

H-b models dealing with irregular waves have only been developed on a statistical basis (Battjes and Janssen (1978), Roelvink & Stive (1989), Dally (1990)). The latest and most advanced of these models (Dally, 1990) assumes the incoming waves follow a Rayleigh distribution and that each wave height is modified through shoaling and breaking as an individual event in time. In particular, near breaking and in the surf zone, this is often a realistic assumption and it makes it possible to determine the changes in the wave height distribution throughout the region.

The difficulty with statistical models is that irregular waves essentially represent time varying wave conditions, which create time varying set-up and currents. This slow time variation is in fact the core of the long wave problems discussed in Section 6. The statistical method cannot predict these phenomena. They essentially assume

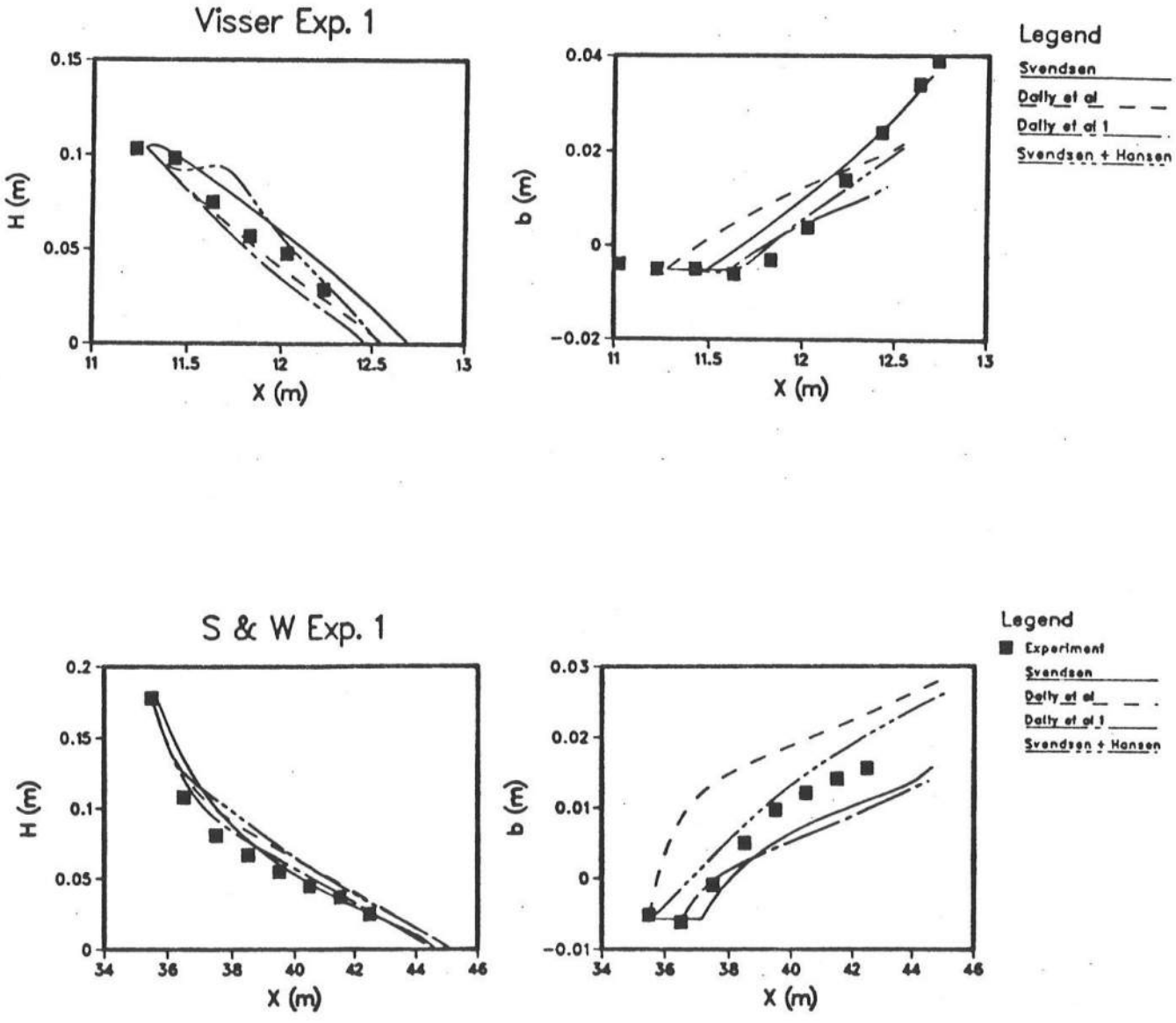

Figure 12: Prediction of wave heights and set-up by H-b models by Svendsen (1984), Svendsen using Hansen's B_0, and the two versions of Dally et al. (1984).

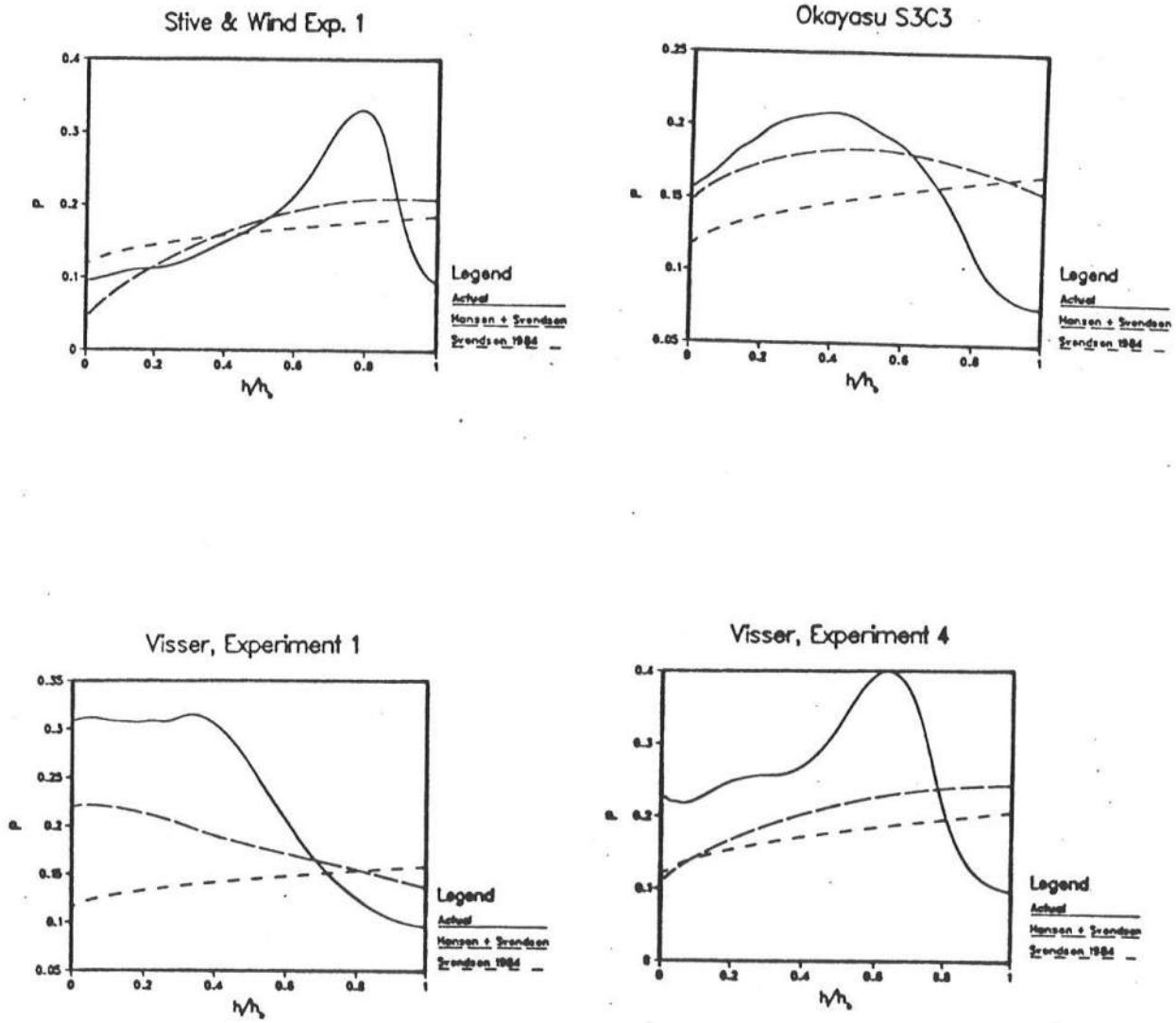

Figure 13: The P-value predicted by (3.10) using $B_0 = 0.65$, and B_0 from Hansen (1990) (Eqs. 3.1–3.5) for Stive & Wind Experiment No. 1

an equilibrium solution exists for each wave frequency or individual wave. The statistical solution is then established as the average of all these equilibrium solutions. Hence, statistical methods are unable to predict both the actual time variation of a wave situation and the complicated long wave phenomena in a realistic manner. Since the surf zone response to irregular (time-varying) waves is the result of highly nonlinear processes, the best approach to these problems will be to analyze them as an actual time series. If a statistical description is wanted for the resulting phenomenon, it may be obtained by a direct statistical analysis of the resulting time series for the phenomenon in question. This, however, has not been done yet.

4.3 Time Domain Models

Wave models in the full time domain have primarily been based on the non-linear shallow water (NSW) equations. Normally, these equations predict incorrectly that all waves break, even on a constant depth. This means that they cannot be used to predict the prebreaking behavior of the waves, including where the waves will break. However, numerical solutions of the equations using the special dissipative Lax-Wendroff scheme artificially freeze the wave fronts once the waves are breaking and compensate for this by a numerical dissipation which equals that of a hydraulic jump or bore of the same height as the wave. Thus a simplified version of the surf zone motion can be modelled this way though the realism of the wave shape and particle velocity field is somewhat limited. The method has been utilized by Hibberd and Peregrine (1979) and later by Kobayashi and co-authors to study broken waves particularly on steep slopes (such as structures) and in the swash zone. These models can analyze irregular waves as a time series (Kobayashi, et al. 1990). They also seem to give useful results for waves in the swash zone which is a region not covered by the H-b models or other models.

An extension of the NSW-model to include the effect of turbulence and avoiding the above mentioned deficiencies of the ordinary NSW model was developed by Svendsen and Madsen (1984) but only for a single bore incident on a beach.

5 NEARSHORE CIRCULATION

Nearshore circulation is the term for the currents created by the breaking waves, and basically the governing equations are the depth integrated, time averaged equations for conservation of mass momentum and energy shown in Section 2.

The understanding of nearshore circulation dates from the realization of the fact discussed above that water waves represent a mean momentum flux, the radiation stress, and derivation of the wave averaged momentum equation already shown in section 2 (Longuet-Higgins and Stewart, 1960 and subsequent publications). As mentioned in Section 4, Longuet-Higgins and Stewart (1963) used this to predict the setdown of nonbreakng waves, and Bowen et al. (1968) measured and computed set-up in the surf zone. The analysis of set-up inside the surf zone was also discussed in Section 4.

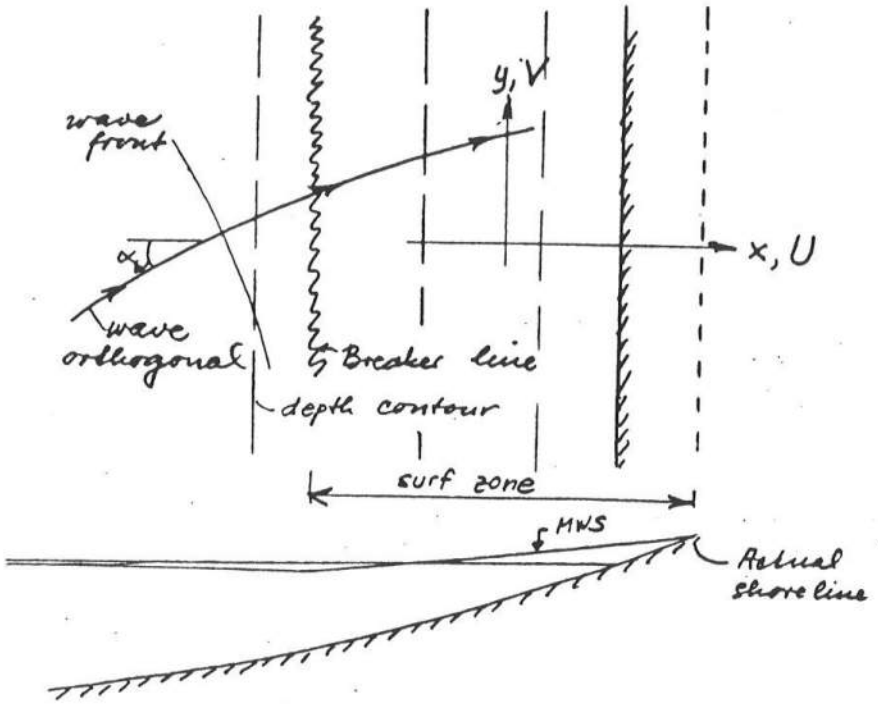

Figure 14: Longshore current generation on a long straight coast.

obtained by substituting (5.3) into (5.2).

Bottom Shear Stress

The mean bottom friction τ_y^B in (5.1) is the effect of a complicated interaction between waves and longshore currents in the boundary layer near the bottom. The following expression was used for weak currents and waves nearly perpendicular to the currents

$$\tau_y^B = \frac{1}{\pi} \rho f u_o V \tag{5.5}$$

where u_o is the bottom velocity amplitude in the waves, f an empirical friction factor. This expression is based on the assumption that the mean shear stress τ_α^B can be written as

$$\overline{\tau_\alpha^B} = \frac{1}{2} \rho f \overline{[U_\alpha + u_{w\alpha}(t)|U_\alpha + u_{w\alpha}(t)|]} \tag{5.6}$$

Liu & Dalrymple studied various other cases of $\overline{\tau_\alpha^B}$ derived from this formulation such as strong currents, and Svendsen and Putrevu (1990) showed that in general $\overline{\tau_\alpha^B}$ obtained from (5.6) can be written

$$\overline{\tau_\alpha^B} = \frac{1}{2} \rho f u_o \{V_\alpha \beta_1 + u_{o\alpha} \beta_2\} \tag{5.7}$$

where β_1 and β_2 are functions of $u_o = |u_{o\alpha}|$ and $V_b = |V_\alpha|$ and of the angle μ between the wave and the current directions. The variation of β_1 and β_2 is shown in Figs. 15 for the case where

$$u_{w\alpha} = u_{o\alpha} \cos \omega t \tag{5.8}$$

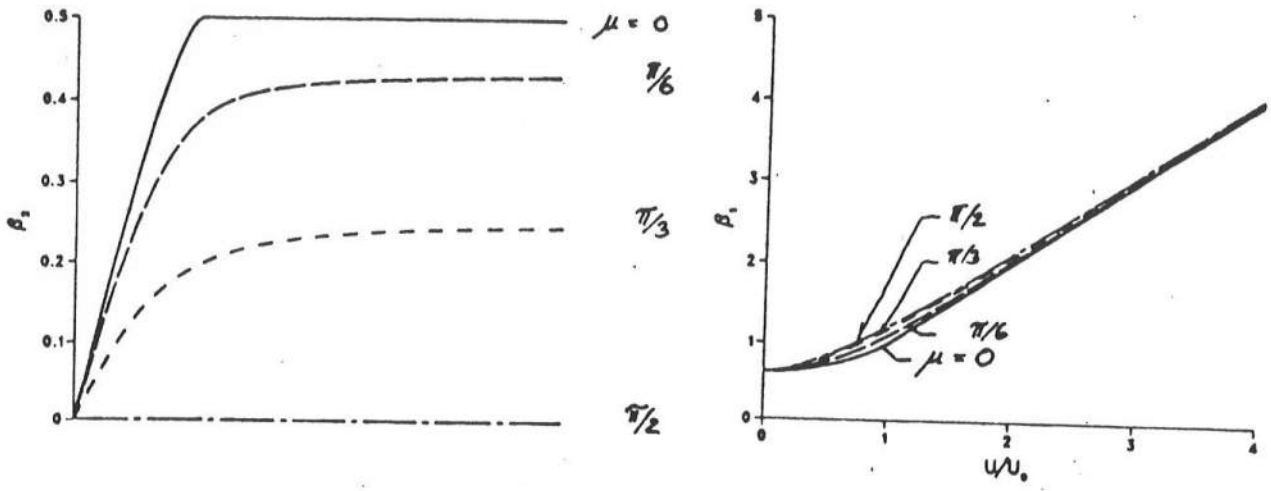

Figure 15: β_1 and β_2 (from Svendsen & Putrevu, 1990).

Results for Longshore Currents

Thus by substituting all these results into Eq. (5.1), that equation can be written

$$\frac{d}{dx}\left(\nu_t h \frac{dV}{dx}\right) - \frac{1}{\pi} f u_o V = \frac{1}{\rho}\frac{dS_{xy}}{dx} \tag{5.9}$$

which is a differential equation for the longshore current $V(x)$ driven by dS_{xy}/dx.

Longuet-Higgins (1970) used linear wave theory also inside the surf zone to approximate S_{xy}. This leads to the solution to (5.9) shown in Fig. 16. The solution contains the parameter

$$P = -2\pi \frac{N h_x}{\gamma f} \tag{5.10}$$

where $\gamma = H/h = \text{const}$ and N is a constant in the expression

$$\nu_t = N \frac{h}{h_x}\sqrt{gh} \tag{5.11}$$

used for the eddy viscosity ν_t.

We see that P expresses the relative strength between the turbulent mixing (measured by N) and the bottom friction (measured by f).

Fig. 16 shows that for $P = 0$ (no mixing), there will be no longshore current outside the surf zone. This is a consequence of the fact that $d\,S_{xy}/dx = 0$ for nonbreaking waves (i.e., outside the surf zone) on a straight coast as shown for periodic potential waves of arbitrary height by James (1974).

A large number of improvements and generalizations of this theory have been published since 1970. Of particular interest is the fact that the values of the eddy viscosity ν_t required to make the theory fit experimental data such as Visser (1982, 84) has turned out to be much larger than what can be defended by turbulence measurements (Svendsen & Putrevu, 1990). This suggests that mechanisms other than turbulent mixing are

the character of a circulation in the vertical plane: substantial amounts of water are carried shoreward as mass transport in the breaking waves and this volume is returned as the seaward going undertow currents essentially below trough level of the waves. These currents (the undertow) have been found to be very strong, generally 8–10% of $\sqrt{gh}$ near the bottom. The mechanism was described qualitatively by Dyhr-Nielsen and Sorensen (1970) and analyzed by Svendsen (1984b).

The forces driving the undertow are caused by the uneven distribution over depth of the two main terms in (4.2). This equation tells us that in the steady case, a gradient db/dx on the mean water level is established to create a pressure force $\rho\, g(h_0 + b)\, db/dx$ that balance the decrease in dS_{xx}/dx in radiation stress. This balance, however, is in average over the depth. However, since the contributions to these two mechanisms are differently distributed over the vertical a (seaward oriented) net force will act on each fluid particle below wave trough level and this drives the undertow. Fig. 17 shows this mechanism.

Since the first analysis, Dally and Dean (1984), Hansen and Svendsen (1984), Stive and Wind (1986), Svendsen et al. (1987), Okayasu et al. (1988) and Deigaard and Fredsoe (1989) have, among others, contributed further to the explanation of the phenomenon.

Thus, Hansen & Svendsen (1984) speculated that the higher turbulent intensities in the main part of the water column produced by the breaking relative to the weak boundary layer turbulence and damping of the breaker turbulence near the bottom causes the (mainly oscillatory) bottom boundary layer to act as a low friction lubrication layer that allows higher velocity shear for the same shear stress than in the rest of the water column. Using two (very) different, but constant eddy viscosities in the two regions, Svendsen et al. (1987) showed that this was indeed true and could account for the remarkably high undertow velocities measured close to the bottom.

Fig. 18 shows the situation. Okayasu (1988) proposed a linear eddy viscosity variation over depth and Deigaard et al. (1991) used a one equation model to determine ν_t. Furthermore, the disturbance of the wave motion by variation of depth and wave height will modify the shear stress distribution (the effect of wave height variation was addressed by Deigaard and Fredsoe, 1989).

Finally, it is noted that the cross-shore circulation and particularly the seaward oriented undertow is thought to be instrumental in coastal erosion during heavy storms.

3-D Currents

The simultaneous existence of cross-shore and longshore currents together combine to form a vertical distribution of wave generated currents in the surf zone which has a spiral shape as shown in Fig. 19. This was analyzed by Svendsen and Lorenz (1989) and Svendsen and Putrevu (1990).

General Circulation Model

In cases of longshore (as well as cross-shore) variations in bottom topography, the net cross-shore flows need not be zero and horizontal circulation patterns such as rip currents can develop.

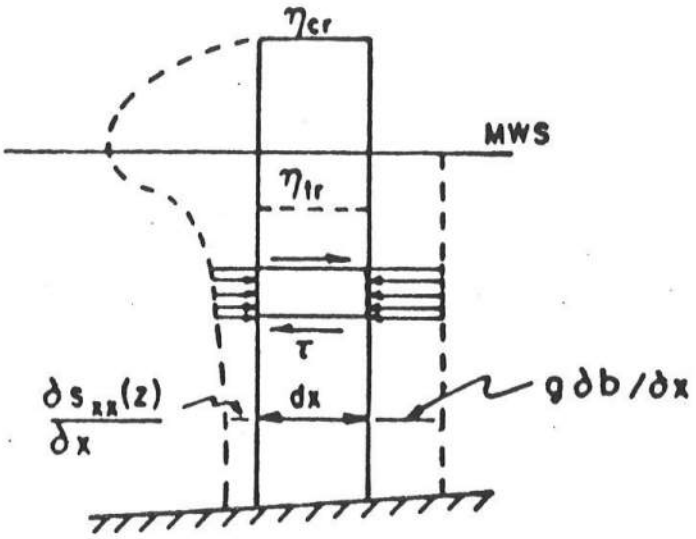

Figure 17: The forcing mechanism for undertow (from Svendsen, 1984b)

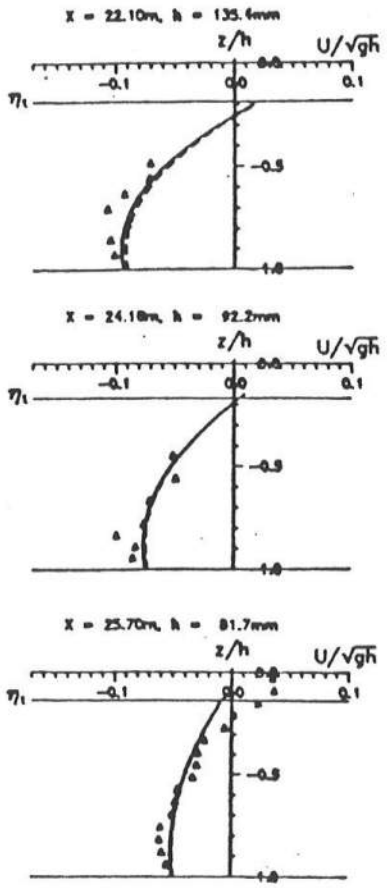

Figure 18: Experimental and computed undertow velocities (from Hansen & Svendsen, 1987)

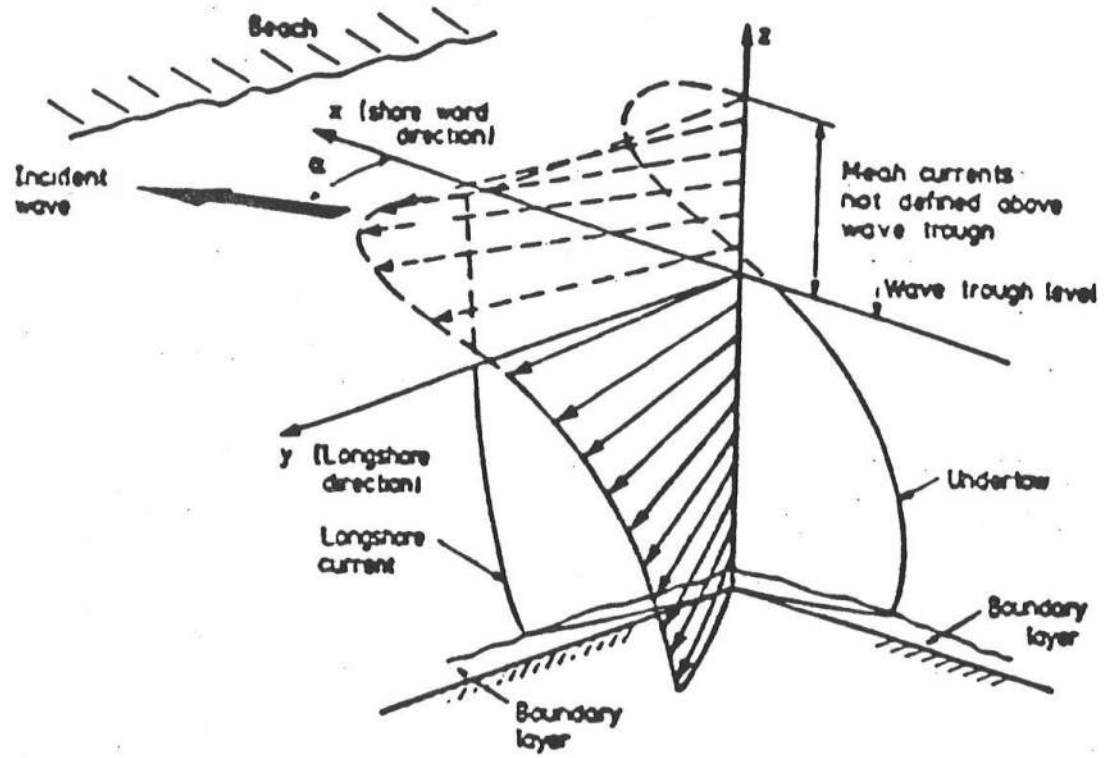

Figure 19: The three dimensional structure of surf zone current profiles (from Svendsen & Lorenz, 1989).

This was acknowledged early and a large number of comprehensive circulation models were developed. Based on purely depth averaged equations (and hence neglecting the undertow and cross-shore circulation in the vertical plane), these models analyze only net flows. In its most general form, such a model encompasses

(a) A wave propagation model that determines wave patterns due to topography and geometry (refraction, diffraction, interaction with structures) and predicts wave height variation, including breaking.

(b) A current generation model component based on the wave-averaged momentum equation.

However, models capable of dealing with all these phenomena have yet to be developed. In the earlier models, the wave component (a) was limited to specifying linear shoaling outside breaking and $H = \gamma h$ (saturated breaker) inside the surf zone with γ constant or given by Miche's formula. Refraction was incorporated using Munk and Arthur's (1952) theory for ray tracing (Noda, 1972, 1974) or limiting the models to long straight coasts and using Snell's law (Birkemeier and Dalrymple, 1976; Ebersole and Dalrymple, 1979). Later models often use more advanced models for the pattern of wave propagation but still the simple saturation model for the wave height inside the surf zone.

A few recent examples are Watanabe (1985) (modified mild slope equation) and Winer (1988) (parabolic wave model with energy dissipation).

6 INFRA-GRAVITY WAVES

Long waves (or infra-gravity waves) are waves with significantly longer period than the peak frequency of the incident wave spectrum. Field measurements show that such waves occur very frequently and different mechanisms have been considered for their generation. One is resonant interaction between ordinary waves (Gallagher, 1971; Bowen and Guza, 1978). Another is the effect of wave height variation in the incident wave trains, sometimes called "surf beat" (Munk, 1949; Symonds et al., 1982; Schaffer and Svendsen, 1988).

The long waves occur both as waves bound to the incident wave train and as free waves which develop by either direct energy transfer from the short wave train or are formerly bound waves released from the short wave train by changes in that wave train due to shoaling and breaking. The free waves are often trapped along the coast as edge waves. Numerous references are omitted here for brevity.

Basic Equations

The strongest of the above mentioned long wave generation mechanisms is the variation of wave height and period of incident storm waves or swell. This causes a similar variation in the radiation stress of these waves which acts as a forcing of (long) "setdown waves" with length and period as the variation in the radiation stress of the incoming waves. Inside the surf zone, these waves become "set-up waves."

This mechanism can be modelled by the depth integrated, wave averaged equations of Section 2 in sufficiently shallow water, by considering these waves as time and space varying currents with velocity Q_x/h and with surface elevation $b(x_\alpha, t)$.

The continuity equation remains as (2.12)

$$\frac{\partial b}{\partial t} + \frac{\partial Q_\alpha}{\partial x_\alpha} = 0$$

In the momentum equation (2.13), the primary terms are the inertia, the gradient on the mean water surface and the radiation stress gradient. Thus (2.13) simplifies to

$$\frac{\partial Q_\alpha}{\partial t} + g h_o \frac{\partial b}{\partial x_\alpha} = -\frac{1}{\rho} \frac{\partial S_{\alpha\beta}}{\partial x_\beta} \tag{6.1}$$

From (2.12) and (6.1), we may eliminate Q_α to get the following equation for b

$$\frac{\partial^2 b}{\partial t^2} - \frac{\partial}{\partial x_\alpha}\left(g h_o \left(\frac{\partial b}{\partial x_\alpha}\right)\right) = \frac{1}{\rho} \frac{\partial^2 S_{\alpha\beta}}{\partial x_\alpha \, \partial x_\beta} \tag{6.2}$$

where $S_{\alpha\beta}$ is supposed known from the short wave motion. b will represent the surface variation of the long waves. Note that $S_{\alpha\beta} = S_{\alpha\beta}(x_\alpha, t)$ because the shore wave height varies in space and time.

(6.2) is actually an inhomogeneous version of the mild-slope equation for long waves, which corresponds to $S_{\alpha\beta} = 0$. The complete solution of (6.2) is a combination of free waves (homogeneous solutions) and forced waves (inhomogeneous solutions).

Edge Waves

Among the homogeneous solutions to (6.2) we find edge waves which is a class of waves that propagate largely along the shore and with amplitudes that decrease rapidly in the seaward direction.

Analytical solutions are known for these waves on a long straight beach. To find these solutions, we consider the homogeneous version of (6.2), (written in coordinate form for convenience).

$$\frac{\partial^2 b}{\partial t^2} - \frac{\partial}{\partial x}\left(gh_o \frac{\partial b}{\partial x}\right) - \frac{\partial}{\partial y}\left(gh \frac{\partial b}{\partial y}\right) = 0 \tag{6.3}$$

and seek solutions of the form

$$b(x, y, t) = \eta(x) \exp(i(k_y y - \omega t)) \tag{6.4}$$

Substitution of (6.4) into (6.3) leads after some changes (see e.g., Mei, 1983) to the following equation for $\eta(x)$

$$x\eta'' + \eta' + \left(\frac{\omega^2}{gh_x} - xk_y^2\right)\eta = 0 \tag{6.5}$$

It turns out that (6.5) has solutions of the form

$$\eta = e^{-k_y x} f(2k_y x) \tag{6.6}$$

where f is a confluent hypergeometric function, but the physically realistic solutions require that

$$\omega^2 = gk_y(2n+1)h_x \tag{6.7}$$

when n is a positive integer. This is the long wave version of the general edge wave dispersion relation. With $h_x = \tan\beta$, β - the beach slope angle - (6.7) compare well with the general dispersion relation (arbitrary wave lengths) which reads

$$\omega^2 = gk_y \sin[(2n+1)\beta] \tag{6.8}$$

particularly for gently sloping beaches. This general solution was given by Ursell (1952).

The solutions that satisfy (6.7) are edge waves of order n. Fig. 20 shows the variation of the surface elevation of the lowest order edge waves in the shore normal direction, normalized relative to their vertical amplitude at the shoreline. It is noted that since the shore parallel propagation speed c_y equals ω/k_y we have

$$c_y^2 = \frac{g}{k_y}(2n+1)h_x \tag{6.9}$$

which can be compared with the deep water propagation speed c_0

$$c_0^2 = g/k_y \tag{6.10}$$

for waves of the same length. We see that for $(2n+1)h_x \ll 1$ we have $c_y \ll c_0$.

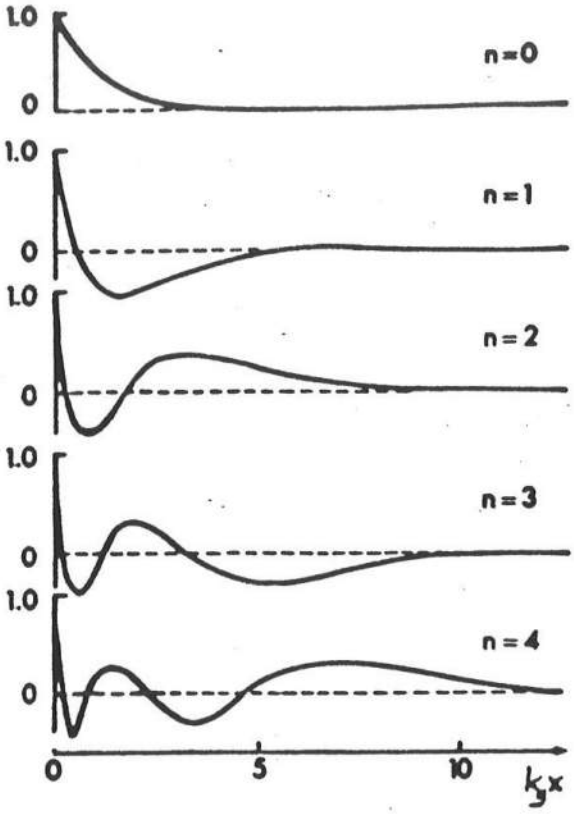

Figure 20: Variation of edge wave amplitude $\eta(x)$ in the shore normal direction (modified from Mei, 1983)

Forced Long Waves

The forced solutions to (6.2) have only been partly explored for the simple case of shore normal wave motion.

Thus Symonds et al. (1982) analyzed the generation of long waves by the variation of the break point which occurs due to a simple periodic variation in the height of the incident short waves ("groupiness"). Schaffer and Svendsen (1988) studied the generation of long waves by groupiness outside and inside the surf zone. The two assumptions were combined by Schaffer (1990) who also studied edge waves forced by these mechanisms.

7 VERY LONG PERIOD WAVES, SHEAR WAVES

Recently, some field experiments have shown signs of very long period oscillations in the horizontal velocity field (Tang and Dalrymple, 1988; Oltman-Shay et al., 1989). These oscillations are of relative shore length and propagate along the shore at a speed comparable to that of the longshore current. Hence their propagation speed is lower than even low order edge waves. They have been attributed to instabilities in the longshore current (Bowen and Holman, 1989) but the phenomenon is still under investigation.

Alternative explanations for these observations have been suggested by Fowler & Dalrymple (1990) and Shemer et al. (1991).

8 REFERENCES

Banner, M.L. (1987). "Surging characteristics of spilling zones on quasi-steady breaking water waves," in Horikawa & Maeno, *Nonlinear Water Waves*, IUTAM Symp., Springer, Tokyo.

Basco, D.R. and T. Yamashita (1986). "Toward a simple model of the wave breaking transition region in surf zone," *20th ICCE*, Taipei, Chap. 72, 955.

Battjes, J.A. (1975). "Modeling of turbulence in the surf zone," *Proc. Symp. on Modeling Techniques*, San Francisco, 1050–1061.

Battjes, J.A. and T. Sakai (1981). "Velocity field in a steady breaker," *J. Fluid Mech.*, **111**, 121–137.

Battjes, J.A. and J.P.F.M. Janssen (1978). "Energy loss and set-up due to breaking of random waves," *Proc. 16th ICCE*, Hamburg, Chap. 32, 569–587.

Birkemeier, W.A. and R.A. Dalrymple (1976). "Numerical models for the prediction of wave set-up and nearshore circulation," *Ocean Eng. Rep. 3*, Dept. of Civil Engineering, University of Delaware.

Bowen, A.J. (1969). "The generation of longshore currents on a plane beach," *J. Marine Res.*, **27**, 206–215.

Bowen, A.J. and R.A. Holman (1989). "Shear instabilities of the mean longshore current. 1. Theory," *J. Geophys. Res.*, C12, 18023–18030.

Bowen, A.J. and R.T. Guza (1978). "Edge waves and surf beat," *J. Geophys. Res.*, 83, 1913–1920.

Bowen, A.J., D.L. Inman and V.P. Simons (1968). "Wave 'set-down' and set-up," *J. Geophys. Res.*, **73**, 2569–2577.

Dally, W.R. (1990). "Random breaking wave: A closed form solution for planar beaches," *Coast. Eng.*, **14**, 233–263.

Dally, W.R. and R.G. Dean (1984). "Suspended sediment transport and beach profile evolution," ASCE, **110**, WW1, WPCOE, 15–33.

Dally, W.R., R.G. Dean and R.A. Dalrymple (1984). "A model for breaker decay on beaches," *Proc. 19th Conf. Coast. Eng.*, Houston, 82–98.

Dally, W.R., R.G. Dean and R.A. Dalrymple (1985). "Wave height transformation across beaches of arbitrary profile," *J. Geophys. Res.*, 11917–11927.

Deigaard, R. (1989). "Mathematical modelling of waves in the surf zone," *ISVA Prog. Rep. 69*, Technical University of Denmark, 47–60.

Deigaard, R. and J. Fredsoe (1989). "Shear stress distribution in dissipative water waves," *Coastal Eng.*, **13**, 4, 357–378.

Deigaard, R., P. Justesen and J. Fredsoe (1991). "Modelling of undertow by a one equation turbulence model," *Coastal Eng.*, **15**, 431–458.

Duncan, J.H. (1981). "An experimental investigation of breaking waves produced by a towed hydrofoil," *Proc. Roy. Soc. Lond.*, **A377**, 331–348.

Dyhr-Nielsen, M. and T. Sorensen (1970). "Sand transport phenomena on coasts with bars," *Proc. 12th Int. Conf. Coast. Eng.*, Ch. 54, 855–866.

Ebersole, B.A. and R.A. Dalrymple (1979). "A numerical model for nearshore circulation including convective acceleration and lateral mixing," *Ocean Eng. Rep. 21*, Dept. of Civil Engineering, University of Delaware.

Fowler, R.E. and R. A. Dalrymple (1990). "Wave group forced nearshore circulation," *Proc. 22nd Int. Conf. Coast. Eng.*, Ch. 56, 729–742.

Gallagher, B. (1971). "Generation of surf beat by nonlinear wave interactions," *J. Fluid Mech.*, **49**, 1–20.

Galvin, C.J. (1968). "Breaker type classification on three laboratory beaches," *J. Geophys. Res.*, **73**, 12.

Hansen, J.B. (1990). "Periodic waves in the surf zone: Analysis of experimental data," *Coastal Eng.*, **14**, 14–41.

Hansen, J.B. and I.A. Svendsen (1984). "A theoretical and experimental study of undertow," *Proc. 19th Int. Conf. Coast. Eng.*, Houston, Ch. 151, 2246–2262.

Hansen, J.B. and I.A. Svendsen (1987). "Surf zone breakers with a current," *Proc. IUTAM Symp. on Nonlinear Waves*, Tokyo.

Hattori, M. and T. Aono (1985). "Experimental study of turbulence structures under spilling breakers," in *The Ocean Surface*, Toba and Mitsuyasu, eds., Reidel Publ. Comp., Dordrecht, 419–424.

Hibberd, S. and D.H. Peregrine (1979). "Surf and runup on a beach: A uniform bore," *J. Fluid Mech.*, **95**, 323– 345.

James, I.D. (1974). "A non-linear theory of longshore currents," *Est. & Coast. Mar. Science*, **2**, 235–249, Part 2.

Jansen, P.C.M. (1986). "Laboratory observations of the kinematics in the aerated region of breaking waves," *Coast. Eng.*, **9**, 5, 453–477.

Kobayashi, N., D.T. Cox and A. Wurjanto (1990). "Irregular wave refraction and run-up on rough impermeable slopes," *WPCOE*, ASCE, **116**, 6, 708–726.

Liu, P.L-F. and R.A. Dalrymple (1978). "Bottom frictional stresses and longshore currents due to waves with large angles of incidence," *J. Marine Res.*, **36**, 2, 357–375.

Longuet-Higgins, M.S. (1970). "Longshore currents generated by obliquely incident sea waves, 1 & 2," *J. Geophys. Res.*, **75**, 6778–6789 & 6790–6801.

Longuet-Higgins, M.S. (1973). "A model of flow separation at a free surface," *J. Fluid Mech.*, **57**, 1, 129–148.

Longuet-Higgins, M.S. and R.W. Stewart (1960). "Changes in the form of short gravity waves on long waves and tidal currents," *J. Fluid Mech.*, **8**, 565–583.

Longuet-Higgins, M.A. and R.W. Stewart (1963). "A note on wave set-up," *J. Mar. Res.*, **21**, 4–10.

Longuet-Higgins, M.S. and J.S. Turner (1974). "An 'entraining plume' model of a spilling breaker," *J. Fluid Mech.*, **63**, 1, 1–20.

Mei, C.C. (1983). "The Applied Synamics of Ocean Surface Waves," Wiley Interscience.

Munk, W.H. (1949). "Surf beats," EOS, *Transactions of the American Geophysical Union*, **30**, 849–854.

Munk, W.H. and R.S. Arthur (1952). "Wave intensity along a refracted ray in gravity waves," *Nat. Bur. Stand. Circ. 521*, Washington, D.C.

Nadaoka, K. (1986). "A fundamental study on shoaling and velocity fluid structure of waver waves in the nearshore zone," Ph.D. Diss., Dept. of Civ. Eng., Tokyo Inst. of Tech.

Noda, E.K. (1972). "Rip currents," *Proc. 13 ICCE*, Vancouver, Chap. 35, 653–668.

Noda, E.K. (1974). "Wave induced nearshore circulation," *J. Geophys. Res.*, **79**, 4097–4106.

Okayasu, A. (1989). "Characteristics of turbulence structures and undertow in the surf zone," Ph.D. Diss., Univ. of Tokyo.

Okayasu, A., T. Shibayama and K. Horikawa (1988). "Vertical variation of undertow in the surf zone," *Proc. 21 ICCE*, Ch. 33, 478–491.

Okayasu, A., T. Shibayama and N. Mimura (1986). "Velocity field under plunging waves," *Proc. 22nd Int. Conf. Coast. Eng.*, Chap. 50, 660–674.

Oltman-Shay, J., P.A. Howd and W.A. Birkemeier (1989). "Shear instabilities of the mean longshore current, *J. Geophys. Res.*, **94**, C12, 18031–18042.

Peregrine, D.H. and I.A. Svendsen (1978). "Spilling breaker, bores and hydraulic jumps," *Proc. 16th ICCE*, Hamburg, Ch. 30, 540–550.

Phillips, O.M. (1977). "The Dynamics of the Upper Ocean," Cambridge Univ. Press.

Putrevu, U. and I.A. Svendsen (1991). "Wave induced nearshore currents: A study of the forcing, mixing and stability mechanisms," *Center for Applied Coastal Research Report CACR-91-11*, Dept. of Civil Engineering, University of Delaware.

Roelvink, J.A. and M.J.F. Stive (1989). "Bar generating cross shore flow mechanisms on a beach," *J. Geophys. Res.*, **94**, C4, 4785–4800.

Schäffer, H.A. (1990). "Infragravity waves induced by short wave groups," Series Paper 50, Institute of Hydrodynamics and Hydraulic Eng., Tach. Univ. of Denmark.

Schäffer, H.A. and I.A. Svendsen (1988). "Surf beat generation on a mild slope beach," *Proc. 21st ICCE*, Chap. 79, 1058–1072.

Shemer, L., N. Dodd and E. B. Thornton (1991). "Sloe-time modulation of finite-depth non-linear water waves: Relation to longshore current oscillations," *J. Geophys. Res.*, **96**, C4, 7105–7113.

Stive, M.J.F. (1980). "Velocity and pressure field of spilling breakers," *Proc. 17th ICCE*, Chap. 34, pp. 547–566.

Stive, M.J.F. (1984). "Energy dissipation in waves breaking on gentle slopes," *Coastal Eng.*, **8**, 99–127.

Stive, M.J.F. and H.G. Wind (1982). "A study of radiation stress and set-up in the nearshore region," *Coastal Eng.*, **6**, 1, 1–26.

Stive, M.J.F. and H.G. Wind (1986). "Cross-shore mean flow in the surf zone," Coastal Eng., **10**, 325–340.

Svendsen, I.A. (1984a). "Wave heights and set-up in a surf zone," *Coastal Eng.*, **8**, 303–330.

Svendsen, I.A. (1984b). "Mass flux and undertow in a surf zone," *Coastal Eng.*, **8**, 4, 347–365.

Svendsen, I.A. (1987). "Analysis of surf zone turbulence," *J. Geophys. Res.*, **92**, C5, 5115–5124.

Svendsen, I.A. and R.S. Lorenz (1989). "Three dimensional velocity profiles in combined undertow and longshore currents," *Coastal Eng.*, **13**, 1, 55–80.

Svendsen, I.A. and P.A. Madsen (1981). "Energy dissipation in hydraulic jumps," ISVA Prog. Rpt. 55, 39–47.

Svendsen, I.A. and P.A. Madsen (1984). "A turbulent bore on a beach," *J. Fluid Mech.*, **148**, 73–96.

Svendsen, I.A., P.A. Madsen and J. Buhr Hansen (1978). "Wave characteristics in the surf zone," *Proc. 16th ICCE*, Chap. 29, 520–539.

Svendsen, I.A. and U. Putrevu (1990). "Nearshore circulation with 3D profiles," *22 ICCE*, Chap. 18, 241– 254.

Svendsen, I.A., H.A. Schäffer and J.B. Hansen (1987). "The interaction between the undertow and the boundary layer flow on a beach," *J. Geophys. Res.*, **92**, C11, 11845–11856.

Symonds, G., D.A. Huntley and A.J. Bowen (1982). "Two dimensional surf beat: Long wave generation by a time-varying breakpoint," *J. Geophys. Res.*, **87**, C1, 492–498.

Tallent, J.R., T. Yamashita and Y. Tsuchiya (1989). "Field and laboratory investigation of large scale eddy formation by breaking water waves," in *The Water Wave Kinematics*, Torum, A. & O.T. Gudmestad, eds. NATO ASI Series E: Applied Science, Vol. 178, 509–523.

Tang, E. and R.A. Dalrymple (1988). "Rip currents and wave groups," in *Nearshore Sediment Transport*, R.J. Seymour, ed., Plenum Publishing Corp., 205–230.

Thornton, E.G. and R.T. Guza (1986). "Surf zone longshore currents and random waves: Field data and models," *J. Phys. Oceanography*, **16**, 7, 1165–1177.

Thornton, E.G. (1970). "Variation of longshore current across the surf zone," *Proc. 12th ICCE*, Washington, D.C., Chap. 18, 291–308.

Ursell, F. (1952). "Edge waves on a sloping beach," *Proc. Roy. Soc. A*, **214**, 79–97.

Visser, P.J. (1982). "The proper longshore current in a wave basin," *Report No. 82-1*, Dept. Civil Eng., Delft Univ. Technology.,

Visser, P.J. (1984). "A mathematical model of uniform longshore currents and the comparison with laboratory data," *Fluid Mech. Lab. Rep. 84-2*, Delft Univ. Tech.

Watanabe, A. (1985). "Three dimensional predictive models of beach evolution around a structure," *Proc. Water Wave Research*, Hanover, 123–141.

Winer, H.S. (1988). "Numerical modelling of wave-induced currents using a parabolic wave equation," Ph.D. thesis, Dept. of Coast. and Oceanograph. Eng., University of Florida.